An Acad Bras Cienc (2025) 97(Suppl. 1): e20250487 DOI 10.1590/0001-3765202520250487
Anais da Academia Brasileira de Ciências | *Annals of the Brazilian Academy of Sciences*
Printed ISSN 0001-3765 I Online ISSN 1678-2690
www.scielo.br/aabc | www.fb.com/aabcjournal

PALEONTOLOGY

Taphonomic analysis of *Thanatosdrakon amaru* (Pterodactyloidea: Azhdarchoidea) and paleoenvironmental reconstruction of the Plottier Formation (Upper Cretaceous, Neuquén Basin), Mendoza, Argentina

LEONARDO D. ORTIZ-DAVID, BERNARDO J. GONZÁLEZ-RIGA, GABRIEL CASAL, MARÍA BELÉN TOMASELLI & IMANOL FIGUEREDO-VIEYRA

Abstract: The fossil remains of *Thanatosdrakon* from the Plottier Formation (PS-3 quarry, Mendoza, Argentina) offer a unique opportunity to investigate the preservation of pterosaurs in fluvial environments. The objective of this study is to reconstruct the taphonomic history of the holotype (UNCUYO-LD 307) and paratype (UNCUYO-LD 350). Detailed stratigraphic analysis together with taphonomic attributes allowed defining that the specimens were preserved with a variable drainage floodplain taphonomic mode (VDF-BA). Distinct taphonomic submodes were defined for each specimen, reflecting differences in biostratinomic and fosildiagenetic processes. The holotype, which was discovered in reddish pelites interpreted as floodplain deposits, exhibits associated skeletal elements suggesting rapid burial. In contrast, the paratype, composed of only one humerus, exhibits evidence of prolonged subaerial exposure, which is evidence that it was exposed to different paleoenvironmental conditions. These findings underscore the variable preservation pathways within the same depositional setting and highlight the influence of both rapid burial and prolonged exposure on the fragile skeletons of large pterosaurs. The taphonomic submodes that have been defined contribute valuable insights into the taphonomic biases that have shaped the pterosaur fossil record in the Cretaceous Patagonian basins.

Key words: Thanatosdrakon, Taphonomy, Azhdarchid, Cretaceous.

INTRODUCTION

The fossil record shows that pterosaurs were extremely diverse animals in both their morphology and their feeding habits. As discussed in Smith et al. (2023) and references therein, they colonized a great diversity of ecosystems and achieved a wide global distribution. With more than 200 taxa known around the world, pterosaurs have been found in diverse sedimentary facies interpreted as fluvial environments, freshwater and salt lakes and lagoons, open sea, and deserts. However, pterosaur fossils are often quite unusual relative to the record of other contemporary vertebrates that inhabited the same environments (such as turtles, crocodiles, and dinosaurs). In a comprehensive analysis on the preservational bias in the pterosaur record, Dean et al. (2016) concludes that–in a general sense–pterosaur remains are often highly fragmentary and provide little paleobiological information, and that the pterosaur fossil record is strongly biased by the occurrence and distribution of Lagerstätten deposits. Kellner (1994) proposed

five sites susceptible to being considered as Lagerstätten deposits for pterosaurs worldwide. These sites are 1) the Norian associations in Italy, Austria and Switzerland in Europe, 2) the Upper Jurassic Solnhofen Formation in Germany, 3) the Yixian and Jiufotang formations of the Lower Cretaceous of China, 4) the Romualdo, Santana and Crato formations of the Lower Cretaceous in Brazil, and 5) the Upper Cretaceous Niobrara Formation deposits in the United States (Witton 2013, and references therein).

By their very nature, Lagerstätten-type deposits represent a limited number of environments with well-defined characteristics, which generates a narrow view of the preservation conditions of pterosaurs. This limitation highlights the necessity for in-depth analysis of deposits that do not fall within the scope of this special type of preservation. Conversely, the fragility of pterosaur skeletons could provide an explanation for the scarcity of remains in various fossil vertebrate sites (Witton 2013, Ortiz-David 2019). However, these issues have ever been conducted. The aforementioned inquiries underscore the significance of pterosaurs as a subject of inquiry for taphonomic studies. These studies endeavor to elucidate the processes involved in the preservation of pterosaur skeletons in disparate environments that diverge from Lagerstätten-type deposits. In summary, taphonomic studies gain relevance in complementing the information of taxa with interpretations linked to the environments they inhabited and how they were preserved. As mentioned by Behrensmeyer et al. (2000), taphonomy constitutes a tool that integrates biological, sedimentological, ecological, and evolutionary observations. On the other hand, taphonomic studies on pterosaurs (like those of other Mesozoic vertebrates) do not present a significant development when compared to other types of studies focused on anatomy, morphological diversity, phylogeny, histology, paleoecology, and biomechanics (Unwin 2003, 2005, Kellner 2003, 2010, Lü et al. 2009, Andres et al. 2014, Witton & Naish 2008, Barrett et al. 2008, Hone & Henderson 2014, Bestwick et al. 2018, 2020, Chatterjee & Templin 2004, Habib 2008, Palmer & Dyke 2010, Naish & Witton 2017, Palmer 2018, Padian 1983, de Ricqlès et al. 2000, Williams et al. 2021). Only a few works on these archosaurs develop taphonomic studies or include a taphonomic section in their analyses (Nessov 1991, Kellner 1994, Frey & Martill 1994, Kemp 1999, 2002, Vremir et al. 2013, Beardmore et al. 2017, Ortiz-David et al. 2019c, Lehman 2021, Smith et al. 2023). In this context, the present contribution stands out, aiming to analyze the biostratinomic, fossildiagenetic, and paleoenvironmental aspects of the provenance site of *Thanatosdrakon amaru* to clarify the preservation process, establish taphonomic modes, and the taphonomic history of this taxon. The information presented herein provides a robust foundation for subsequent paleoecological interpretations, particularly in the context of comparisons with the record of other species in South America.

MATERIALS AND METHODS

Thanatosdrakon is a taxon composed of two specimens designated under the acronyms UNCUYO-LD 307 (holotype) and UNCUYO-LD 350 (paratype). The holotype represents one of the best-preserved giant azhdarchids in the world due to the conservation of various axial and appendicular elements with very good three-dimensional preservation (Table I). These remains were recovered from a single site of approximately 8 m^2. A comprehensive study of the aforementioned fossil materials was conducted in several works, including a Ph.D. thesis (Ortiz-David unpublished data), articles in

Table I. Axial and appendicular elements of *Thanatosdrakon amaru*.

Holotype UNCUYO-LD 307	
UNCUYO-LD 307-1	incomplete posterior cervical vertebra
UNCUYO-LD 307-2	notarium formed of five fused vertebrae and one rib
UNCUYO-LD 307-3 to 6	four free dorsal vertebrae
UNCUYO-LD 307-7	synsacrum formed of three fused vertebrae
UNCUYO-LD 307-8	two incomplete sacral vertebrae
UNCUYO-LD 307-9	complete caudal vertebra
UNCUYO-LD 307-10	right scapulocoracoid
UNCUYO-LD 307-11	right humerus
UNCUYO-LD 307-12	proximal portion of right ulna
UNCUYO-LD 307-13	proximal portion of right radius
UNCUYO-LD 307-14	left proximal syncarpal
UNCUYO-LD 307-15	left distal sincarpal
UNCUYO-LD 307-16	right pteroid
UNCUYO-LD 307-17	distal portion of wing metacarpal
UNCUYO-LD 307-18	proximal and distal portion of wing phalanx 1
UNCUYO-LD 307-19	distal portion of right wing phalanx 2
UNCUYO-LD 307-20	proximal portion of left wing phalanx 3
UNCUYO-LD 307-21	distal portion of right wing phalanx 3
UNCUYO-LD 307-22	proximal portion of right wing phalanx 4
UNCUYO-LD 307-23	left pelvis
UNCUYO-LD 307-24	proximal portion of right femur
UNCUYO-LD 307-25	distal end of fused right tibiotarsus
Paratype UNCUYO-LD 350 - left humerus	

scientific journals (Ortiz-David et al. 2018, 2022a) and published meeting abstracts (Ortiz-David et al. 2019a, b, c, 2021a, b, 2022b, 2024). These works encompassed anatomical, phylogenetic, paleohistological, ontogenetic and taphonomic analyses. The detailed anatomical description of both specimens is currently in the process of being published.

The stratigraphic sections of the Plottier Formation that are exposed at the Agua del Padrillo-Cerro Guillermo Norte sector were measured in detail. The orientation of the fossil remains (strike and dip) as well as paleocurrent directions were measured using a Brunton compass. The nomenclature of Miall (1996) was employed for the analysis of facies and fluvial architecture.

For the taphonomic study, the following attributes were analyzed: a) weathering was assessed using the stages described by Behrensmeyer (1978); b) integrity and type of fractures were determined following the proposal of Alcalá (1994) and Tomassini et al. (2010); c) transport, orientation, articulation, and dispersion following the definitions and methodologies proposed by Behrensmeyer (1991); d) impregnations and color, as defined by Tomassini et al. (2010); e) abrasion, bioerosion,

encrusting, and element density, as proposed by Fernández-López (2000) and Behrensmeyer (1991); and f) plastic deformation, as measured by Casal et al. (2013, 2014).

The number and types of fractures in the incomplete remains were determined by considering the angle formed between the fracture and the anteroposterior medial axis of the element. According to Tomassini et al. (2010), three types of fractures were considered: longitudinal (angles between 0° and 29°), oblique (angles between 30° and 59°), and transverse (angles between 60° and 90°). To measure plastic deformation in vertebral elements, the detailed proposal by Casal et al. (2013, 2014) was followed. According to this method, the deformation can be dimensioned by considering the shear angle (ψ) and the shear value (γ), where the shear value is the tangent of the shear angle. Finally, the taphonomic modes (*sensu* Behrensmeyer & Hook 1992) were analyzed following the proposal and nomenclature of González Riga et al. (2022).

Geological setting

The Jurassic and Cretaceous sedimentary sequences of the southern Mendoza province are part of the Neuquén Basin, which is located on the eastern side of the Andes in Argentina. This basin, which spans an area of over 120,000 km^2 (Yrigoyen 1991), features a continuous record of up to 4,000 m in thickness. This succession corresponds to the Late Triassic–Early Cenozoic period. It includes siliciclastics, carbonates and evaporates facies that accumulated during a complex sedimentary history (Barrio 1990). Throughout much of its history, the basin has been constrained on its northeastern and southern margins by extensive cratonic areas of the Sierra Pintada Massif and the North Patagonian Massif, respectively. The westernmost margin of this basin corresponds to the Andean magmatic arc, situated along the active western margin of the Gondwanan–South American Plate (Howell et al. 2005).

The paleontology of the Neuquén Basin is of significant global importance due to its rich record of both marine invertebrates and continental vertebrates. The basin has been found to contain one of the most comprehensive records of Jurassic and Cretaceous marine invertebrate faunas. This record has enabled the construction of accurate biostratigraphic charts for western Gondwana (e.g., Aguirre-Urreta et al. 1999, Riccardi et al. 1999). In a similar vein, the Mesozoic continental and marine reptile record is regarded as one of the most complete, varied, and well-preserved globally (Gasparini et al. 1997, 1999, Leanza et al. 2004, Calvo et al. 2011)

However, among fossil vertebrates, pterosaurs are relatively scarce, with the notable exception of *Thanatosdrakon*, which represents the largest flying reptile in South America and exhibits exceptional preservation (Ortiz-David et al. 2018, 2022a).

The Neuquén Group, deposited between the early Cenomanian (97 ± 3 Ma) and the early Campanian (74 ± 3 Ma) periods, constitutes a sequence within the basin that reaches a thickness of up to 1,200 m. This sequence is delineated at its base and apex by the Patagonidican and Huantraiquican unconformities, respectively (Cazau & Uliana 1973, Leanza & Hugo 1997). We follow the proposal by Garrido (2010) for the formations of the Neuquén Group.

These siliciclastic sequences are indicative of fluvial systems, with certain sections exhibiting characteristics of aeolian, lacustrine, and playa lake facies. However, alluvial fans predominate towards the basin's border. As is common in red beds, the lateral changes of fluvial facies make it difficult to correlate different formations and members (González Riga & Astini 2007). However, detailed stratigraphic studies in southern Mendoza Province (Paso de las Bardas,

Cerro Guillermo, and Agua del Padrillo sectors) have allowed the identification of different formations and facies sequences, particularly those associated with dinosaur quarries (González Riga 2002).

The Plottier Formation (Coniacian–Santonian) is characterized by an alternating and variable succession of sandy and pelitic facies, indicative of fluvial systems and extensive muddy floodplain deposits, both well- and poorly-drained. The presence of extensive outcrops has been documented in various sectors of southern Mendoza Province, including Paso de Las Bardas, Cerro Guillermo, and Agua del Padrillo. These locations have been noted for their abundance of dinosaur and other vertebrate fossils (Figure 1a).

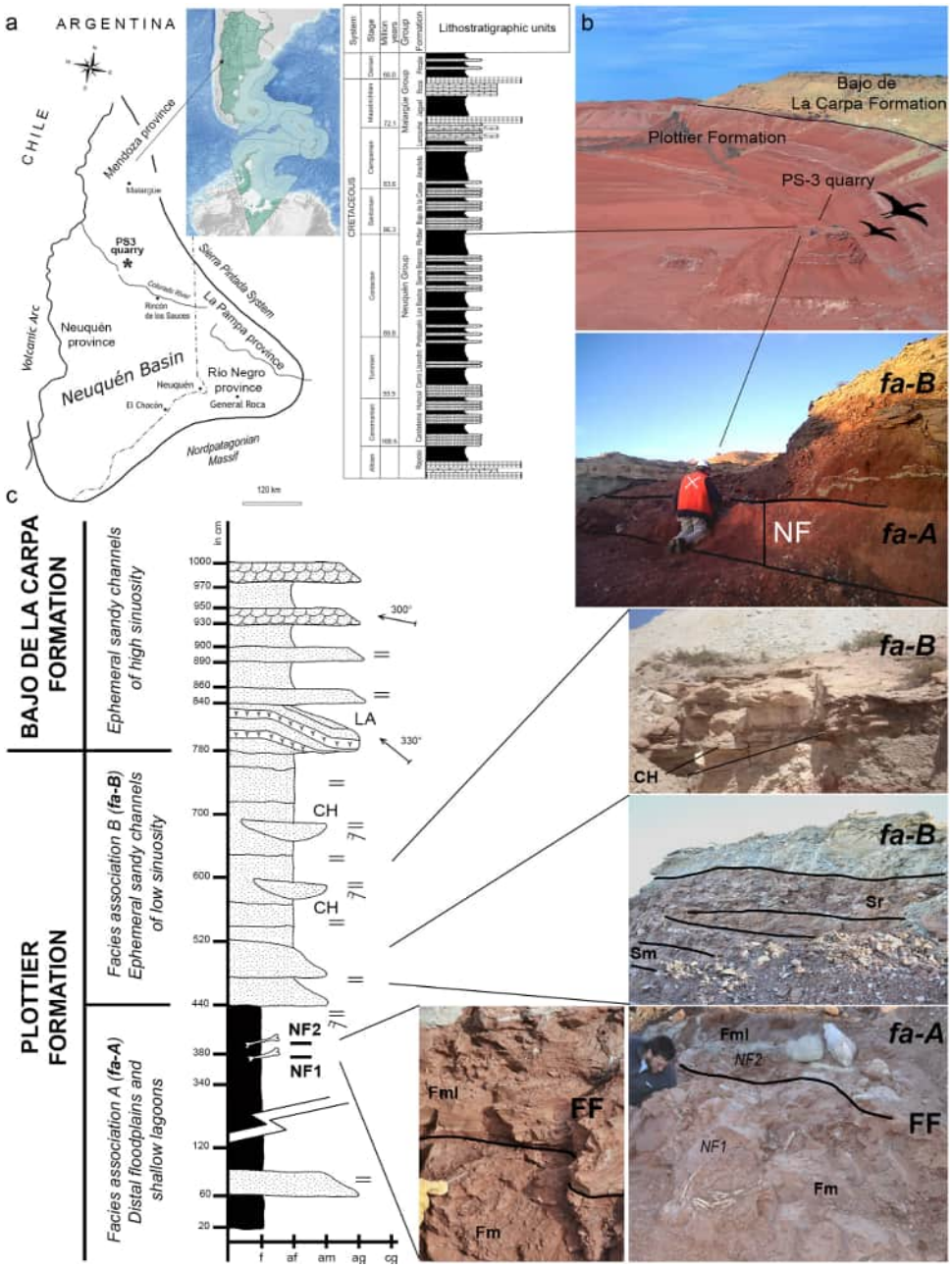

Figure 1. (a) Map of the Neuquén Basin showing the location of the PS-3 quarry and stratigraphic column of the Neuquén Groups. (b) General view of the PS-3 quarry in the Agua del Padrillo Sector, Malargüe, Mendoza Province. (c) Detailed stratigraphic profile of the upper section of the Plottier Formation, showing facies association, architectural elements and fossiliferous levels. Abbreviations, NF: Fossiliferous Level, LA: Lateral Accretion, CH: Fluvial Channel, FF: fine floodplain deposits, Fm: mudstones and siltstones, Fml: laminated mudstones with ripples, Sr: ripple cross-laminated sandstones, Sm: sandstones with massive structures.

Thanatosdrakon specimens described herein were found in the upper section of the Plottier Formation, approximately 8 km from the quarry of the titanosaur *Notocolossus*, one of the largest dinosaurs discovered in the world (González Riga et al. 2016). In addition, other specimens of titanosaur were unearthed in the aforementioned formation. Some of these specimens were articulated and exhibited exceptional preservation, including articulated feet and an almost complete skull. These specimens were also found in association with theropods, turtles, and crocodiles (González Riga et al. 2013, 2014a, b). This record indicates the paleontological richness of the Agua del Padrillo sector.

RESULTS

Stratigraphic and paleoenvironmental analysis

Thanatosdrakon fossils come from the upper levels of the Plottier Formation. The fossil site, designated PS-3 quarry, is located in a reddish fining-and thinning-upward sequence where the pelitic facies are dominant (Figure 1b). Overlying these strata are coarse to medium yellowish-gray sandy facies of the Bajo de la Carpa Formation (Santonian). In this section, the Bajo de la Carpa and Anacleto Formations are overlain by gray Pleistocene basaltic conglomerates belonging to the Agua Carmona Formation (Holmberg 1976). These dark conglomerates protrude due to differential erosion and form plateaus that crown the reddish-yellow outcrops of the Neuquén Group.

Paleoenvironmental interpretations of the Plottier Formation vary across different sectors of the basin; however, channel belts and broad floodplain deposits are consistently observed (Sánchez et al. 2006, Sánchez & Heredia 2006, Garrido 2010). In the sector studied here, a detailed stratigraphic analysis of the uppermost 25 m, where the PS-3 quarry is located, was performed. Two facies associations, named herein A and B, were recognized (Figure 1c).

Facies Association A (fa-A): It is composed of two different facies. In the lower levels, deep red mudstones and siltstones (Fm) are dominant. Color changes, associated with iron oxidation and reduction, form gray mottles surrounding bone fragments. In the upper levels, laminated mudstones with ripples (Fl) are present. In this case, within the mudstone intervals, disruptions of original sedimentary structures and fabrics occur due to tubular burrowing, infiltrated clay partings, and local abundances of millimeter–centimeter-scale, largely irregular, massive, clay-rich glaebules and calcareous rhizoliths. Here, mudstones are intercalated with silty and fine-sand levels where small ripples are present.

This facies association is interpreted as a progressive decrease in water supply, and therefore, sediment, concomitant with greater subaerial exposure. The Fm was deposited from suspension load in broad floodplains and shallow depth (~ 0.5 m–1 m). The absence of sedimentary structures appears to be primarily due to rapid sedimentation occurring on completely saturated substrates. This is consistent with the absence of soil horizons and desiccation cracks. Fossil remains of the *Thanatosdrakon* holotype (UNCUYO-LD 307) come from this facies and correspond to the fossiliferous level 1 (NF1).

Conversely, facies Fl suggests a substrate with periodic saturation, where episodes of subaerial exposure alternate. In this case, only one isolated humerus, identified as the *Thanatosdrakon* paratype (UNCUYO-LD 350) has been recovered. It belongs to a larger specimen of the same species and come from to the fossiliferous level 2 (NF2). Although both facies correspond to fine floodplain deposits (FF *sensu* Miall 1996), differences between them indicate

changes in some conditions. First, facies Fm corresponds to swamps formed in poorly drained alluvial plains. Subsequently, facies Fl indicates a slight change in water supply conditions, where suspension processes are intercalated with tractive currents of low flow regime (ripples preserved in fine sandstones). In this case, the alteration of parallel lamination by burrowing organisms, the infiltrated textures (product of illuviation), and the local presence of globules and rhizoliths suggest a preliminary development of soils. It is evident that the bones left on these substrates here may have undergone subaerial exposure. For more data about the development of soils, detailed micromorphological and geochemical studies are required (Retallack 2001).

Facies Association B (fa-B): It includes a reddish fining-and thinning-upward sequence formed by two main architectural elements. One of them is composed of fine-grained, reddish sandstones that lie as thin, tabular bodies (~0.2 m thick). They have ripple cross-laminated sandstone (Sr), parallel lamination (Sh), and massive structures (Sm). Alternating with these bodies is also present another element. It has concave erosional bases lens (~5 m wide and 0.4 m thick) interpreted as channels (CH element). They are composed of fine to medium-sized sandstones with planar cross-bedding (Sp) generated by the migration of 2-D dunes. This facies association contains some internal scour surfaces, indicating the common occurrence of high-energy, shallow flow near the transition from subcritical to supercritical. This association of facies is interpreted as flash flood deposits and episodic and ephemeral low-sinuosity channels. The channels are amalgamated and cut each other, with changes in the runoff direction.

Contact with the overlying formation: The Bajo de la Carpa Formation shows a reactivation of the fluvial system. It presents tabular bodies of medium to coarse yellowish sandstones (0.20-0.80 m thick) with marked lateral accretion (LA, 'epsilon' bedding). In some strata, fibrous gypsum layers (1-5 cm thick) occur, accompanying the bedding and covering the roof of the silicoclastic facies. Above this, medium to coarse laminated sandstone facies develop, with trough cross-bedding (ST). The lithological contact between the Plottier and Bajo de la Carpa Formations is easily recognized by the change in facies, architectural elements, and color.

Taphonomic analyses

This section describes the results of the analysis of the taphonomic attributes present in *Thanatosdrakon*. Linking these attributes to the stratigraphic analyses allowed for the establishment of taphonomic modes and the reconstruction of the taphonomic history of the site.

a - Taphonomic attributes:

Number of individuals and identification

At the PS-3 quarry, bones exhibiting distinct characteristics were discovered, allowing for their preliminary assignment to Pterosauria in the field. No remains of other vertebrates, invertebrates, flora, or trace fossils were found. Subsequent detailed analyses led to the erection of a new taxon named *Thanatosdrakon amaru* (Ortiz-David et al. 2022a).

The minimum number of individuals was initially estimated based on the repetition of the same skeletal element (*sensu* Alcalá 1994, Cladera et al. 2004, Casal et al. 2014). However, the repetition of other fossil elements was recorded at the site. Consequently, anatomical, taphonomic, and paleoenvironmental criteria

were established to define the total number of individuals.

During the fieldwork, the presence of two pterosaur specimens was established at the PS-3 quarry. These specimens are primarily differentiated by the size of their humeri. Subsequent analyses determined that both humeri exhibit the same anatomical characteristics, leading to the assignment of these materials to the same taxon (Ortiz-David et al. 2018, 2022a, Ortiz-David 2019). However, beyond the size difference, the distinct taphonomic attributes present in each humerus are noteworthy. The UNCUYO-LD 350 humerus displays a deformation not observed in the UNCUYO-LD 307-11 humerus or any other element at the site. The spatial arrangement of the humeri–detailed in the 'Orientation, transport, and dispersion' section–and their preservation suggest the occurrence of differential taphonomic processes at the site. This is further supported by the distinct responses of the two humeri to lithostatic pressures.

To link the remaining preserved elements at the PS-3 quarry with the two specimens defined from the humeri, size relationships between the elements were initially established, revealing that many exhibited similar dimensions or articulated perfectly. Subsequently, size proportions were established and compared with taxa possessing known articulated-associated skeletons. In the initial analysis, it was determined that all elements comprising the axial skeleton belonged to a single individual due to the consistent size among the elements and the morphology of specific structures (i.e., compatible morphology of vertebral centra, correspondence between articular elements, location of the neural canal in the neural arch, location of transverse processes, among others). In particular, it is highlighted that: a) the posterior cervical vertebra is compatible with the first vertebra of the notarium in height and the arrangement of the cotyle-condyle, post-pre exapophyses, post-pre zygapophyses, and neural canal height; b) the 5th dorsal vertebra of the notarium is morphologically similar to the anterior free dorsal vertebrae found, both in the shape and size of structures (such as the vertebral centrum, height of the diapophyses, and location of the neural canal); c) the posterior free dorsal vertebra is morphologically similar to the articulated dorsal vertebrae of the synsacrum (in terms of vertebral centrum morphology, shape and location of the neural canal, neural arch morphology, and location of the diapophyses); and d) the sacral vertebrae exhibit a similar size and shape to the caudal vertebra. Furthermore, the elements maintain spatial relationships in articulation, which strengthens the interpretations.

For their part, the appendicular elements also exhibit connections among themselves, namely: a) correspondence between the size of the glenoid fossa of the scapulocoracoid and the humeral head; b) perfect articulation of the elbow between the humerus and the ulna; c) anatomical correspondence between the ulna and radius; d) perfect articulation between the syncarpals; e) corresponding size between the acetabulum of the pelvis and the femoral head; and f) size of the pelvis in relation to the sacral vertebrae (in this case, following comparisons with articulated specimens such as the azhdarchid indet. MN 6605-v and the indet. specimen MN 6585-v, pers. obs.).

In the second analysis, size proportions between the elements were defined and compared with other taxa. For this purpose, *Quetzalcoatlus northropi* and *Quetzalcoatlus lawsoni* (Andres & Langston 2021) were considered as key taxa. These taxa exhibit a set of characteristics that allow for a certain degree of confidence in the relationships between

elements, such as: a) being composed of diverse remains; b) presenting elements preserved in three dimensions; c) being phylogenetically related to *Thanatosdrakon*; and d) being large-giant azhdarchid pterosaur taxa.

Although interspecific variations and the debated *bauplan* of azhdarchids by various authors (see discussion in Ortiz-David et al. 2022a) were considered, the size relationships between elements serve as a robust indicator for clarifying these taphonomic issues. Similar relative proportions were established between the elements comprising *Quetzalcoatlus* and those of *Thanatosdrakon*. Consequently, all axial and appendicular elements were examined in relation to the proportions of the specimen UNCUYO-LD 307, which consists of the smallest humerus (based on the proportions between: humerus and scapulocoracoid, humerus and syncarpals, syncarpals and the wing metacarpal, wing phalanges and the wing metacarpal, femur and pelvis, and between the vertebrae and some appendicular elements, see Ortiz-David 2019, Ortiz-David et al. 2022a, b). In summary, these analyses allowed for the definition of two individuals belonging to the same pterosaur species at the PS-3 quarry, where the larger specimen is represented only by a complete humerus, while the smaller specimen is represented by a large number of axial and appendicular elements (Figure 2).

Orientation, transport, and dispersion

At the PS-3 quarry, the recovered specimens were found incomplete, disarticulated, and with a reduced horizontal dispersion within an area of approximately 10 m² (Figure 2). Vertical dispersion was also low, as all elements were deposited within a single level of 0.7 m thickness (Figure 1a, 1b). The low hydraulic energy of the distal floodplains generates a low dispersion of the remains due to the low water flow regime, which is evidenced by the limited transport exhibited by the fossils. The degree of disarticulation and the mixing of bones observed at the site suggest that the taphonomic arrangement coincides with the proximity of these structures in life, which is also supported by the limited hydraulic transport of the system. In the taphonomic map of the PS-3 quarry, five groupings of skeletal remains were interpreted:

Group 1: represented by elements of the axial skeleton distributed within an area of 1.30 m². No dispersion of vertebrae beyond these limits occurs at the site, allowing for the definition of this assemblage (Figure 2).

Group 2: represented by elements of the right forelimb (stylopodium and zeugopodium with scapulocoracoid) distributed within an area of 0.90 m². Only the humerus is complete, as the ulna and radius only preserve the proximal epiphysis and a section of the diaphysis. The scapulocoracoid lacks the proximal and distal ends of the scapula and coracoid, respectively (Figure 2g, 2h).

Group 3: represented by the proximal portion of the autopodium, comprising the left proximal and distal syncarpals. These elements were found distributed within an area of 0.30 m² and are associated with other indeterminate elements (Figure 2).

Group 4: represented by the distal portion of the autopodium (right wing phalanges) and the distal portion of the wing metacarpal, distributed within an area of 1.80 m². All elements are incomplete, preserving only one epiphysis and a portion of the diaphysis. The distal end of wing phalanx 1 was found below the notarium, evidencing some movement of the structures within the mudflat where they were deposited (Figure 2c, 2d).

Group 5: comprises posterior appendicular elements, pelvis, femur, and associated fragments, distributed within an area of 0.70 m².

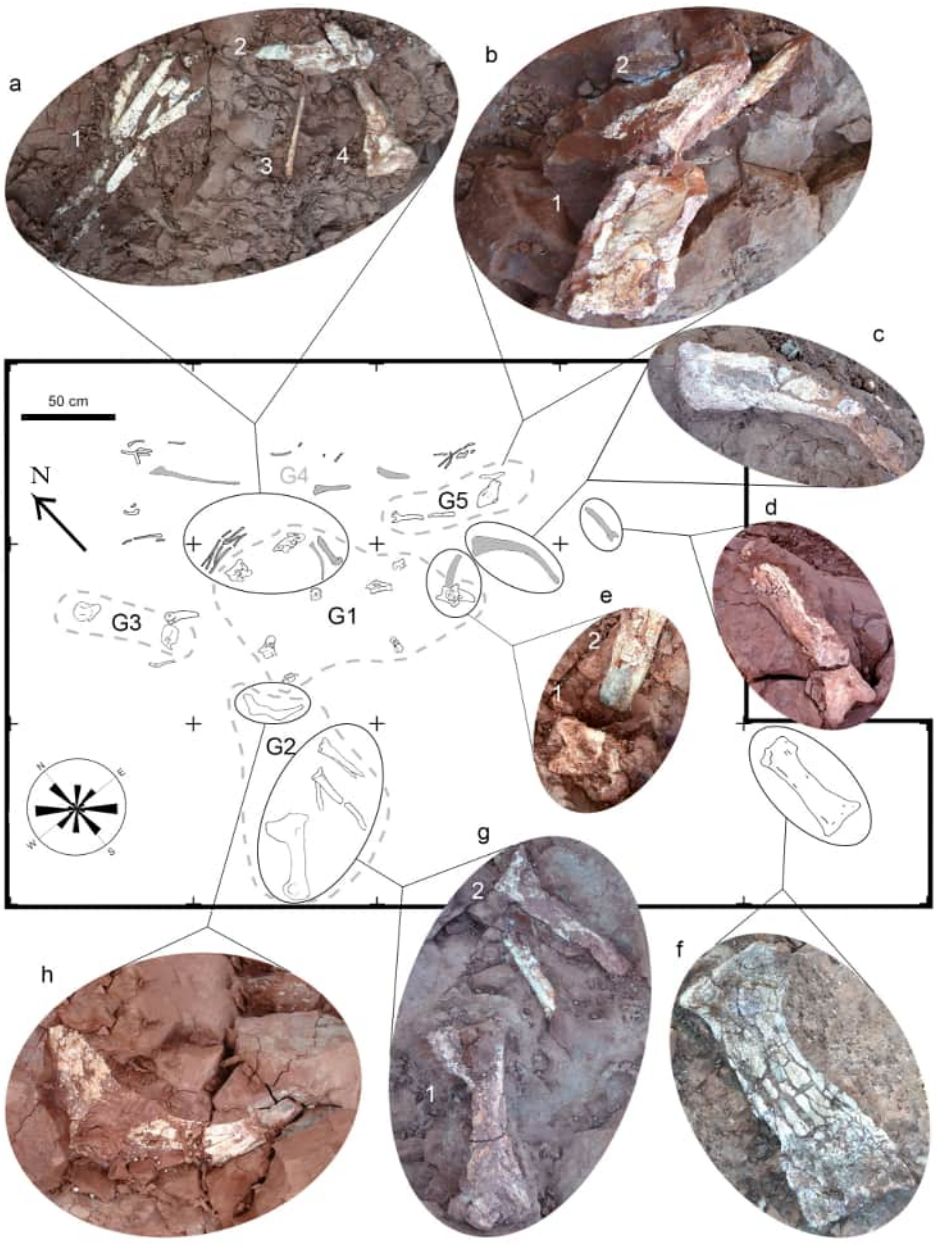

Figure 2. Taphonomic map of the PS-3 quarry, where the analyzed specimens come from, with a circular frequency histogram showing the orientation of the elements. Abbreviations: (a.1) Associated ribs remains, (a.2) synsacrum, (a.3) wing phalanx 4, (a.4) indet. element preliminarily assigned as proximal end of wing metacarpal. (b.1) Pelvis, (b.2) postacetabular process. (c) Wing phalanx 1. (d) Distal end of wing metacarpal. (e.1) Notarium, posterior face of dorsal vertebra V, (e.2) distal end of wing metacarpal. (f) Humerus of specimen UNCUYO-LD 350. (g.1) Humerus of specimen UNCUYO-LD 307, (g.2) radius. (h) Scapulacoracoid. (G1) Group 1 in dashed line. (G2) Group 2 in dashed line. (G3) Group 3 in dashed line. (G4) Group 4 elements colored in gray. (G5) Group 5 in dashed line.

These elements were recovered in an incomplete state, and consistent with other long bones from the site, only a single epiphysis with a partial diaphysis is preserved. Notably, the left pelvis was located 40 cm from the sacral elements, suggesting a potentially weak articulation between these elements, likely involving a significant degree of cartilaginous tissue (Figure 2b).

To determine the spatial distribution (orientation) of the bones, the strike and dip of each element at the site were measured (Table II). Regarding the spatial arrangement of the elements in the bearing layer, the majority were found to be located with their major axis parallel to the surface. The major axis of the appendicular elements is aligned in the proximodistal direction (dip between 0° and 12°), while the major axis of the vertebral elements is situated

Table II. Spatial orientation of the fossil elements of the PS-3 quarry and grouping of identified bones. Measurements of the major axis in millimeters (mm) in the: anteroposterior (a-p), dorsoventral (d-v), and proximodistal (p-d) directions.

Bone grouping	Fossil element	Strike	Dip	Major axis (in mm)
Group 1	Notarium	46° E	90°	107.88 (d-v)
	Cervical vertebra	290° W	19°	108.51 (d-v)
	Free dorsal vertebra I	240° S	90°	90.27 (d-v)
	Free dorsal vertebra III	220° S-W	10°	70.71 (d-v)
	Free dorsal vertebra IV	193° S-W	90°	77.11 (d-v)
	Synsacrum	82° E	18°	86.61 (a-p)
	Sacral vertebrae	98° S-E	3°	70.36 (a-p)
	Caudal vertebra	78° E	12°	52.17 (a-p)
Group 2	Scapulacoracoid	330° W	3°	255.25 (p-d)
	Ulna	352° W	12°	348.45 (p-d)
	Radius	10° E	11°	193.94 (p-d)
	Humerus	43° E	8°	340.18 (p-d)
Group 3	Proximal syncarpal	230° S-W	0°	123.79 (a-p)
	Distal syncarpal	305° W	0°	109.13 (a-p)
Group 4	Wing metacarpal distal	178° S	5°	185.31 (p-d)
	Wing phalanx1 proximal	310° W	42°	401.66 (p-d)
	Wing phalanx 1 distal	270° W	0°	246.24 (p-d)
	Wing phalanx 2 proximal	325° W	6°	165.56 (p-d)
	Wing phalanx 3 proximal	305° W	10°	345.12 (p-d)
	Wing phalanx 3 distal	324° W	5°	182.54 (p-d)
	Wing phalanx 4 proximal	40° E	71°	179.84 (p-d)
Group 5	Pelvis	270° W	42°	149.54 (a-p)
	Femur	250° S-W	35°	143.38 (p-d)

in the dorsoventral direction (dip of 90°). The orientation was represented using a circular frequency histogram, revealing no preferential orientation of the elements. This result aligns with the paleoenvironmental interpretation, wherein scarce and very low-energy water flows prevail. Furthermore, the measured dips support this scenario, with heavier bones sinking into the muddy sediment and acquiring high immersion angles, while lighter elements remained horizontal on the highly viscous, waterlogged substrate exhibiting thixotropic clay properties.

In addition, the spatial distribution of the elements at the site facilitated the development of more precise interpretations related to weathering, deformation, and fracturing processes. The remains of *Thanatosdrakon* were obtained through monitoring and salvage efforts conducted during major civil engineering projects. In this particular context, the fossils were not naturally exposed due to

deformation and tectonism associated with the erosion of outcrops. Rather, the deposits were excavated by heavy machinery and identified by professionals in the field. Consequently, the spatial configuration of the elements was interpreted as it existed at the time of the animal's burial, thereby ruling out the potential influence of exhumation and current erosion.

The notarium was located at the site with its anterior surface facing upwards and exhibits signs of anteroposterior compression. Although this compression generated deformations, the analyses conducted demonstrated that it did not affect the element's morphology, and the anatomical particularities defined therein do not correspond to taphonomic artifacts (Ortiz-David et al. 2023, 2024). Furthermore, prior to burial, the animal's carcass lay on its left lateral side, as evidenced by the weathering indicators on the notarium and synsacrum, which are present on the right lateral side. This characteristic is also observed in the posterior free dorsal vertebra and the anterior free dorsal vertebra.

The analysis of the spatial arrangement of the humeri also strengthened the interpretations of their different taphonomic attributes. Both elements were found in a horizontal orientation at the site, with the ventral surface facing downwards in the case of humerus UNCUYO-LD 350 and the dorsal surface facing downwards in the case of humerus UNCUYO-LD 307-11 (Figure 2f, 2g). While differential lithostatic pressure processes may exist, the proximity of both elements allows us to rule out this hypothesis. It is hypothesized that the humeri exhibited different responses to the same lithostatic pressure, a finding attributed to the pronounced weathering patterns observed in humerus UNCUYO-LD 350 in comparison to those observed in humerus UNCUYO-LD 307-11 (refer to the relevant section of the present study for further details). The weathering process resulted in the formation of cracks and the degradation of bone tissue, thereby compromising the integrity of the element, and increasing its vulnerability to compression-induced failure.

Finally, the spatial arrangement of the elements is also indicative of the number of individuals, given the observed degree of association and the limited area (~4 m^2) encompassing the elements. These characteristics, in conjunction with the distinctive features of the depositional paleoenvironment –i.e., an ephemeral, poorly drained, and shallow floodplain, devoid of tractive movements of material–, allows us to infer that the animal's carcass retained the elements in a life position for an extended period of time.

Element Density

A total of 42 skeletal elements were recovered from the PS-3 quarry. In the present study, the fused elements and associated fragments were considered as a single element, in order to avoid distortion of the results. Consequently, a density of elements per unit area of 4.2 remains/m^2 was established. In addition, considering the site volume of 7 m^3, a density per unit volume of 6 remains/m^3 was determined. These values indicate a relatively high density, resulting in a significant bone concentration. This finding strengthens previous interpretations, which suggested a restricted transport of the carcasses.

Weathering

The concept of weathering includes all the effects produced in the bone remains as a result of exposure to various factors such as solar radiation, desiccation, alternation of wet and dry periods, among others (Polonio & López-Martínez 2000). This process, which occurs prior to the final burial of the animal carcass, generates clues that allow us to broaden and

strengthen the interpretations of the dominant paleoenvironmental conditions at the site.

Within the context of the PS-3 quarry, the presence of elements that have undergone varying degrees of weathering is evident (Figure 3). This phenomenon has allowed for the identification of the carcass areas that were most exposed to atmospheric factors. Furthermore, these interpretations, linked to the spatial distribution of the elements within a paleoenvironment characterized by limited to no transport, provided additional data for the reconstruction of the taphonomic history of the specimens.

Examination of the axial elements reveals stage 3 and 4 weathering, characterized by significant deterioration that has resulted in the loss of external bone material and has penetrated the structure to a depth of more than 1 mm. Furthermore, considerable cracking with irregularly edged splinters preserved in position within the element has been observed.

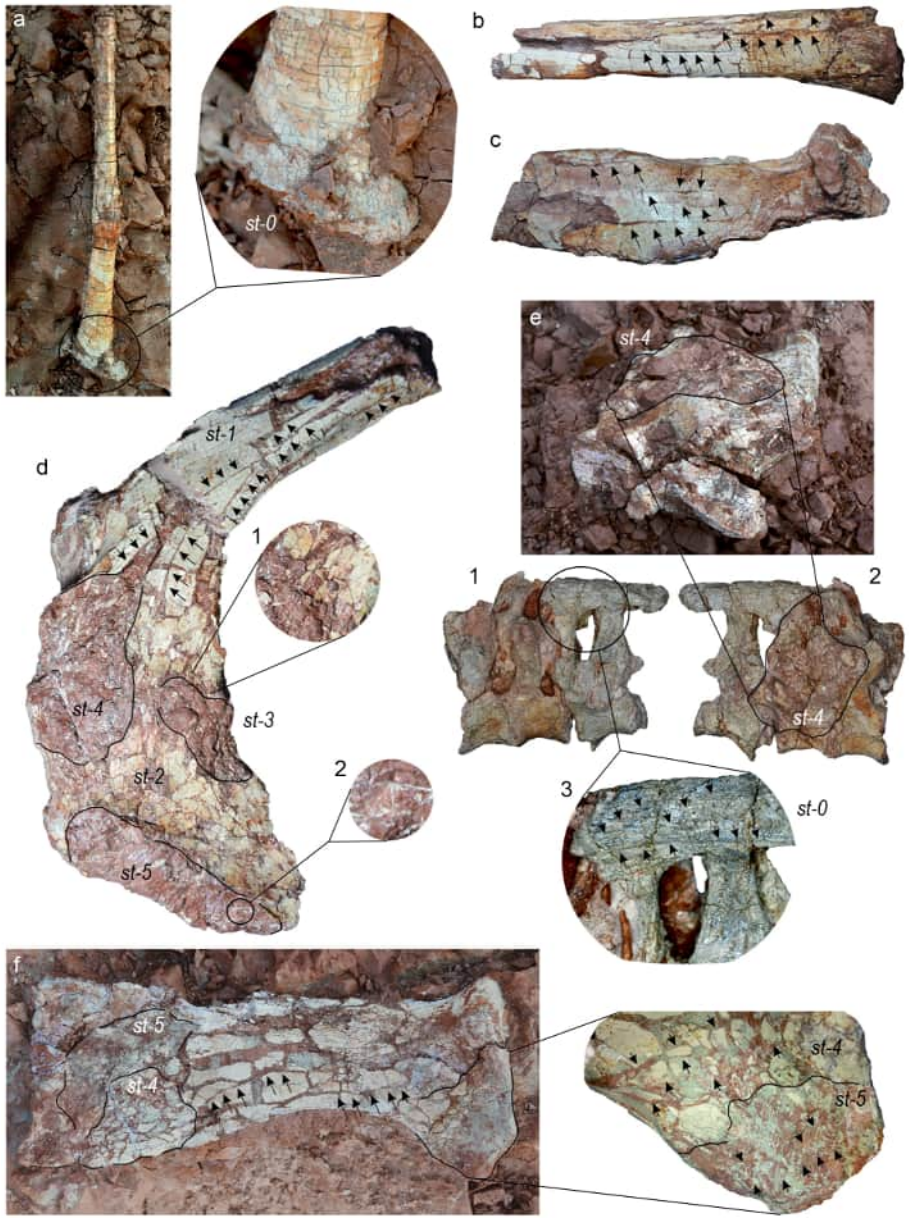

Figure 3. Weathering stages (st) in *Thanatosdrakon* elements (specimen UNCUYO-LD 307). (a) Wing phalanx 4 in situ (with 90° dip in the quarry) with stage 0 weathering (unaltered bone). (b) Wing phalanx 3 with stage 1 weathering (longitudinal and parallel to each other cracks). (c) Femur with stage 1 weathering (longitudinal cracks parallel to each other). (d) Scapulacoracoid with different stages of weathering, (d.1) transition between stage 2 and stage 3 of weathering, where the element shows a step of cracked bone with loss of superficial bone, (d.2) detail of the internal structure of the element due to the complete loss of the cortical bone by weathering. (e) Synsacrum in situ (with dip of 0° in the quarry), (e.1) left lateral of the synsacrum with stage 0 weathering (face downward in the deposit), (e.2) right lateral of the synsacrum with stage 4 weathering (face upward in the deposit), (e.3) detail of the supraneural plate with tendon marks. (f) Humerus of specimen UNCUYO-LD 350 in situ in the quarry with marks of intense weathering and collapse generated by lithostatic compression.

These same weathering stages have been noted on the right lateral and dorsal surfaces of the cervical vertebra, the notarium, the posterior dorsal vertebra, and the synsacrum (Figure 3e). In contrast, the left lateral and ventral regions exhibit remarkable preservation. These observations have been interpreted as an incomplete burial of the carcass, in which a portion of the axial skeleton remained exposed during the decomposition process. The preserved surfaces of the vertebrae show an optimal state of preservation (stage 0 weathering), characterized by the absence of signs of deterioration such as cracks or flaking on the bone surface. Additionally, these vertebrae retain markings originating from soft tissues, such as tendons and ligaments, suggesting significant anatomical integrity (Figure 3e.3).

For their part, the appendicular elements also exhibit different weathering marks (Figure 3b, 3c). The wing phalanges and the femur exhibit stage 1 weathering, as they show cracking parallel to the fibrous structure of the element (longitudinal) running along the diaphyses. These same elements exhibit, on the epiphyses and articular surfaces, mosaic cracking also consistent with stage 1 weathering. However, the scapulocoracoid and an element preliminarily identified as an anterior portion of the sternum present stage 3, 4, and 5 weathering on the same element (Figure 3d.1, 3d.2, respectively). These stages manifest on the surface of the elements as longitudinal cracking associated with flaking and angular striations with loss of osseous material and penetration into the structure of more than 2 mm in depth. Similar stages (3 and 4) were identified on the ventral surface of the humerus UNCUYO-LD 307, which was the exposed side according to its position in the site. Both the scapulocoracoid and the humerus have completely lost part of their structures (i.e., proximal portion of the scapula, distal portion of the coracoid, and ulnar crest of the humerus). On the other hand, there are elements that show no evidence of weathering, such as the syncarpals, the pteroid, the wing phalanx 4, the pelvis, the tibiotarsus, and some free dorsal vertebrae (Figure 3a). The radius and ulna exhibit indications of weathering at stages 2 and 3, with the ventral surface of the ulna epiphysis being the most affected.

The humerus of specimen UNCUYO-LD 350 exhibits indications of weathering at stages 4 and 5 (Figure 3f). On the dorsal face, which was exposed on the surface prior to burial, there is cracking in different directions, chipping of the cortical bone, and deep tissue loss accompanied by flaking, which generates an irregular and rough texture. Weathering has penetrated the cortical structure of the element, affecting it internally. As previously indicated, the severe weathering had an impact on the element's structural integrity, thereby compromising its integrity prior to the process of fossilization. This phenomenon resulted in the failure of the element due to its vulnerability to a loading force induced by lithostatic pressure.

Integrity and fractures

The analysis of the integrity of the preserved skeletal elements was performed by distinguishing between complete elements (i.e., those represented by more than 90% of the element) and incomplete elements. This point is important to mention, since the anatomical fragility the anatomical fragility characteristic of pterosaur remains preserved in facies not belonging to a lagerstätten-type deposit results in incompleteness of all elements. Consequently, only a minimum percentage has been considered complete. This contributes new information to support hypotheses that seek to explain taphonomic biases linked to the low representation of pterosaurs in most continental

sites, where other preserved vertebrates are abundant.

Of the 68 remains that were examined, 6.41% were determined to be complete, while 93.58% were deemed to be incomplete. The distribution of these elements within the site is homogeneous, as evidenced by the taphonomic map. The vertebral elements are the most complete, with four out of nine elements found complete. This phenomenon can be attributed to the intrinsic characteristics of the bone remains, which exhibit an internal spongy tissue and trabeculae that provide greater resistance to lithostatic pressures than hollow bones of the appendicular skeleton. The only appendicular elements that were preserved intact are the syncarpals, which, coincidentally, exhibit a compact structure that differs from that present in the long bones. Furthermore, the humeri of specimens UNCUYO-LD 307 and UNCUYO-LD 350 are the most complete long bones of the appendicular skeleton (Figure 2). These elements are structurally robust due to their morphology, as they are relatively short in relation to the other elements that comprise the wing. The integrity of the appendicular elements is suboptimal, with the preservation of only the epiphysis and a portion of the associated diaphysis.

Regarding fractures, the shape and arrangement of all elements were subjected to analysis. According to several authors (e.g., Polonio & López-Martínez 2000, Cladera et al. 2004), transverse bone fracture can be attributed to a diagenetic origin. This phenomenon can be attributed to the arrangement of fractures, which occur at right angles to the predominant direction of collagen fibers. Consequently, the bone is required to manifest isotropic properties, which are hallmarks of the fossildiagenetic stage, contrasting with the prevailing anisotropic properties that are distinctly evident (Shipman et al. 1981, Alcalá & Escorza 1988, 1998, Polonio & López-Martínez 2000). The elements exhibit an increase in hardness following fossildiagenesis due to the processes of permineralization. However, under stress, they demonstrate a propensity for fragility, attributable to the loss of plasticity in the organic portion of the bone.

In the elements recovered from the PS-3 quarry belonging to specimen UNCUYO-LD 307, fractures were observed, which are mainly transverse. In the case of elements such as the ulna, radius, femur, and wing phalanges, the fractures have sectioned a portion of the diaphysis, displacing it from its original position (Figure 4a). A complete fracture was observed at the junction between the postacetabular process and the ilium in the pelvis (Figure 4b). These anatomical components were found to be associated and in correct position, although fractured. In the wing phalanx 3 and the tibiotarsus, two fractures with a slight displacement of the diaphysis were observed. In the vertebrae of the synsacrum, a fracture with displacement was observed, coinciding with the direction of the compressive stress and consistent with the position of the element in the deposit. This oblique fracture suggests the capacity of the element to resist plastic deformation due to the action of the vertebrae as a compact unit (Figure 4c). This phenomenon is attributed to two factors: the fusion between the elements and the nature of the internal tissue of the vertebral centers. The notarium exhibits an oblique fracture that traverses the structure in its entirety, with no evidence of displacement (Figure 4d).

A phenomenon of particular interest has been observed in the wing phalanx 3, which exhibits a cut in its epiphysis consistent with tectonic displacement, as if the fault plane had traversed the element (Figure 4b). This was analyzed on site and no further information

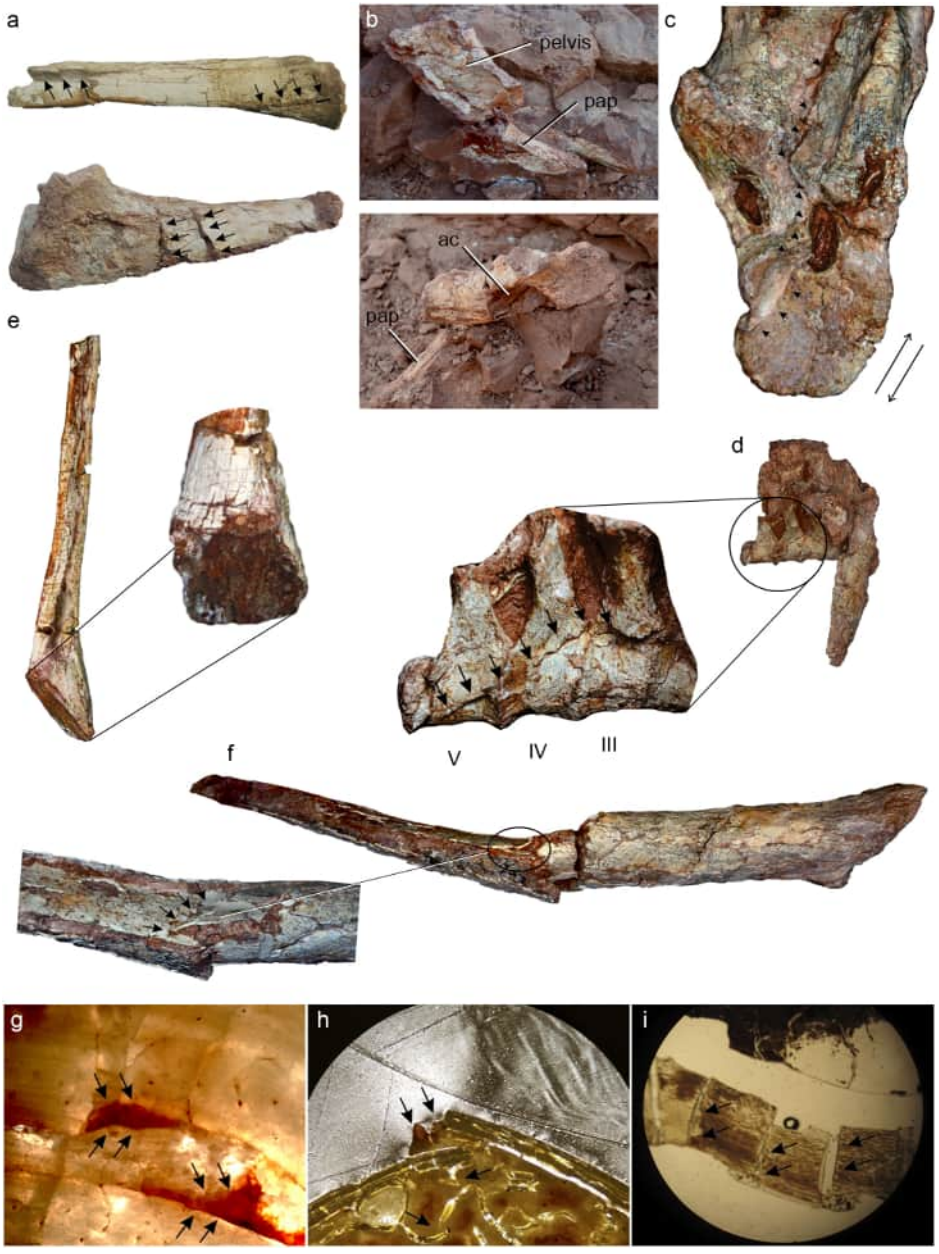

Figure 4. Different fractures present in *Thanatosdrakon* elements (specimen UNCUYO-LD 307). (a) Distal end of wing phalanx 3 and ulna with different transverse fractures. (b) Pelvis in situ showing a complete fracture at the junction of the ilium with the postacetabular process. (c) Sinsacrum in anterior view with an oblique fracture with displacement that crosses the entire element. (d) Notarium in lateral view with a non-displaced oblique fracture crossing the entire element. (e) Wing phalanx 3 showing an epiphysis with a fracture or "cut". (f) Wing phalanx I with fracture and plastic deformation in detail. Microstructure of bones in thin sections of the: (g) diaphysis of wing phalanx III showing vascular channels deformed by lithostatic pressure (200 µm), (h) distal end of the tibiotarsus showing deformed trabeculae and fractured cortical bone (50 µm), (i) cortical bone of the wing metacarpal showing fractures by lithostatic compression (100 µm).

could be obtained, but the element is cut obliquely with slip marks in anterior view.

The humerus UNCUYO-LD 350 exhibits a pattern of fracturing markedly different from that found in all elements of specimen UNCUYO-LD 307, resulting from a diagenetic collapse of the diaphysis (Figure 2f, 2g, 3f). Compressive forces were exerted on the dorsal and ventral surfaces of the element, producing the collapse of the diaphysis and its consequent lateral expansion. The diaphysis lost the medullary cavity, becoming completely flattened, with no evidence of proximodistal expansion of the element. Three types of differential deformation are presented by the element, which allows for the evidencing of how the parts exhibiting greater biological resistance oppose lithostatic deformation. In this element, the following were identified: a) the complete collapse of the diaphysis, which is the least resistant part to compression due

to its completely hollow structure formed only by a layer of tissue a few millimeters thick; b) the deformation of the distal epiphysis, which is expanded laterally (anteroposteriorly), showing the reconfiguration of structures located on the anterior and posterior faces to a ventral plane; and c) the deformation of the proximal epiphysis, which is the least deformed portion of the element and only presents the position of the deltopectoral crest affected, which closes in a U-shape over the element. In the epiphyses, it was observed that the compression did not affect the morphology of the present features (such as the humeral head, deltopectoral crest, ulnar crest, capitulum, trochlea, entepicondyle, and ectepicondyle), as these maintain a morphology similar to that present in the humerus of specimen UNCUYO-LD 307-11 (which is not deformed).

A number of humeri have been identified that exhibit collapse analogous to that observed in this study, characterized by preservation of less deformed epiphyses and completely flattened diaphyses. For instance, *Montanazhdarcho* (McGowen et al. 2002: Fig. 2.C), *Tethydraco* (Longrich et al. 2018: Fig. 2), and *Pteranodon* (Bennett 1993; KUVP 972: Fig. I.B and KUVP 66111: Fig. I.C) have been observed to demonstrate analogous patterns of deformation resulting from lithostatic loading. However, a significant discrepancy is observed in that these elements do not exhibit fracturing or evidence of weathering as the elements studied in this work. Preliminary results indicate that the lithostatic pressures exceeded the maximum load limit that these elements could withstand, resulting in the collapse of their structures. The humerus UNCUYO-LD 350 experienced a collapse due to a significant compromise of its integrity, caused by the intense weathering that weakened its structure and reduced its resistance to pressure. In contrast, the humerus UNCUYO-LD 307-11, located less than three meters away, resisted the lithostatic pressures without evidence of deterioration to its structure.

Finally, a variety of fractures were observed in the elements analyzed through thin sections (Figure 4g, 4h, 4i). This phenomenon can be attributed, at least in part, to the inherent fragility of pterosaur bones, in which the cortical bone constitutes a mere 10-15% of the diaphysis diameter. Conversely, an increase in brittleness is also postulated, attributable to the elevated crystallinity of fluorapatite, as theorized by Casal & Nillni (2020) for vertebrate remains in the Lago Colhué Huapi Formation within the San Jorge Gulf Basin (Central Patagonia, Argentina). Sediments with very fine grain sizes, such as those present during the preservation of *Thanatosdrakon*, are susceptible to greater compaction. Consequently, these sediments would transfer a significant portion of the stresses generated by lithostatic load to the bones. It is noteworthy that the fractured cortical tissue does not exhibit iron minerals, indicating that the brittle fracturing occurred after permineralization, at a greater depth and in a subsequent stage of diagenesis.

Plastic deformation

Prior to the onset of the permineralization process, the elements are subject to acting compressive forces that can generate plastic deformations. At this stage, the bones retain an inherent flexibility attributable to the presence of an organic portion in their structure. The bone, characterized by its ductile nature, undergoes deformation without fracture or failure, thereby adapting its structural integrity to a state of reduced stress (Casal et al. 2007). In this context, a force acting over a prolonged period generates spatial modifications in the remains, that is, a change in the shape and/or location of different structures within the element. This deformation can be analyzed and calculated by comparing

the initial state and the final state of the element under study.

Plastic deformation has been observed in various elements of specimen UNCUYO-LD 307, which exhibit responses to differential compressive forces in accordance with their anatomical resistance. In this regard, the posterior cervical vertebra UNCUYO-LD 307-1 displayed plastic deformation that had modified its structure laterally, deviating the neural arch towards the left flank. This deformation has not affected its height, as the structures of the lateral face are morphologically preserved and without evidence of fractures (Figure 5a). Neither the condyle nor the foramina lateral to the neural canal and the canal itself show signs of dorsoventral elongation of taphonomic origin. The deformation has not modified the shape of the vertebral centrum, which suggests that this part of the element exhibits greater resistance compared to the neural arch. The action of forces on the right lateral face of the element generated deformations in three directions: a) the right lateral apex, situated below the height of the postexapophysis, is posteriorly displaced, deforming the vertebral centrum with a shear angle (ψ) of 10° and a shear strain (γ) of 0.176, observable in both dorsal and ventral views (Figure 5.a.1); b) the neural canal is deviated to the right, presenting, with respect to a normal position (straight conduit in the anteroposterior direction), a ψ = 21° and a γ = 0.383, observable in dorsal view (Figure 5a.2); and c) the neural arch is displaced towards the left flank, with a ψ = 22° and a γ = 0.404, observable in anterior view (Figure 5a.3).

A plastic deformation was observed in the lateral direction of the vertebrae of the synsacrum. This deformation resulted in the reorientation of the right diapophyses, which are oriented posteriorly. In contrast, the normal position observed on the left lateral face is that they project anterolaterally. In this element, the ψ = 42°, the γ = 0.9 and the deformation are observed in dorsal view (Figure 5b).

The limit of plastic deformation of the element prior to fracture was observed in the wing phalanx 1 (Figure 4f). The proximal portion of the diaphysis exhibits a fracture that extends along it in an anteroposterior direction. An exhaustive analysis of the bone layers revealed that the plastic deformation prior to fracturing is still manifested in the bone layers. The evidence obtained from the observation of this peculiar preserved structure suggests a clear correlation between the degree of plasticity of the element and its limit of plastic deformation, which corresponds to a ψ = 12° and a γ = 0.21.

The free dorsal vertebra UNCUYO-LD 307-5 exhibits a substantial degree of plastic deformation, caused by a force acting in a dorsoventral direction, resulting in an alteration and subsequent deviation of the neural arch. The deformation in question presents a ψ = 38° and a γ = 0.78, being observable in the lateral view. The deformation of this element shows a correspondence with its spatial location in the quarry (Figure 5c).

The ulna displays a distinctive morphology on its posterior surface, which is addressed in this section as a preliminary hypothesis suggests that it underwent plastic deformation (Figure 5d). The element displays a cavity that traverses longitudinally the diaphysis up to the olecranon. The cavity is formed by the diaphysis itself, which appears folded, simulating two bones arranged in parallel. Multiple hypotheses related to plastic deformation, fractures, and the orientation of the element within the quarry were evaluated; nevertheless, it proved unfeasible to elucidate this morphology. A thorough review of the extant literature has not revealed any elements that demonstrate similar indications. The structure in question could

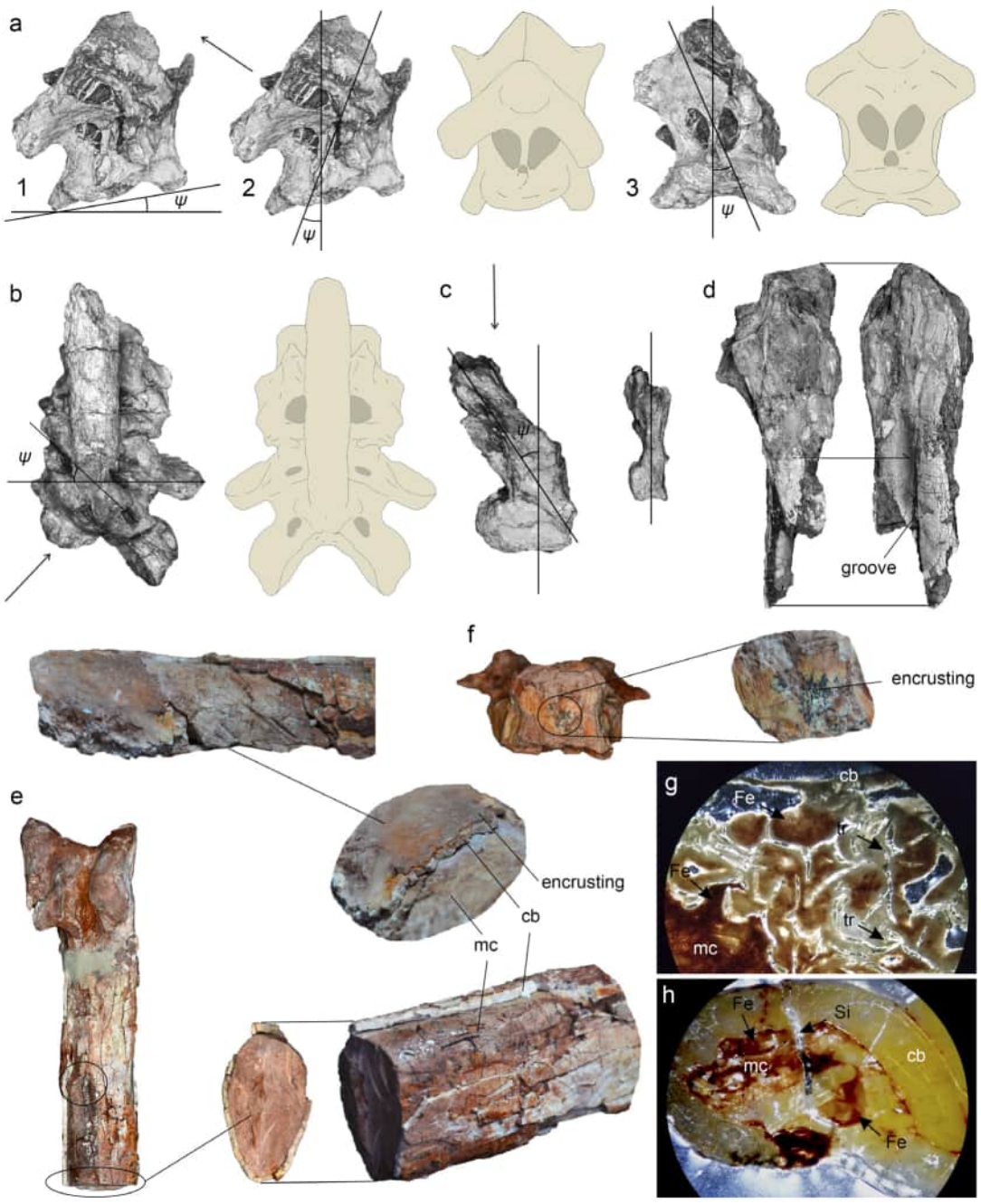

Figure 5. Plastic deformation, encrusting and sedimentary filling in *Thanatosdrakon* elements (specimen UNCUYO-LD 307. (a) Plastic deformation in posterior cervical vertebra, (a.1) deformation in anteroposterior direction, (a.2) deformation in lateral direction, (a.3) deformation in dorsoventral direction. (b) Sinsacrum in dorsal view exhibiting deformation in lateral direction. (c) Free dorsal vertebra III with plastic deformation in dorsoventral direction next to another dorsal vertebra of *Thanatosdrakon* not deformed. (d) Ulna in ventral and posterior view where the particular structure of the longitudinal groove is observed. (e) Distal end of the wing metacarpal in which is indicated: gypsum encrusting, sedimentary filling in the medullary cavity (mc), and cortical bone (cb). (f) Free dorsal vertebra in ventral view with manganese oxide encrusting. Bone microstructure in thin sections of: (g) distal end of the tibiotarsus with primary permineralization between trabeculae (50 µm). (h) diaphysis of wing phalanx III with primary permineralization of iron oxides cut by a fracture with secondary silicate permineralization (50 µm).

have been generated by a plastic deformation process, caused by a specific collapse of the ulna. The spatial location of the element in the quarry, with the ventral side facing upwards, is consistent with a deformation in this sense. However, this structural manifestation is exclusively observed on the posterior surface, while it remains undetectable on the anterior surface. In the doctoral thesis of the first author, it is proposed that the structure corresponds to a morphology associated with the development of the animal and not to a deformation (Ortiz-David 2019). However, further research is necessary to ascertain the origin of this peculiar structure.

The analysis of thin sections from various bone fragments facilitated the identification of plastic deformation in the morphology of the osteons, resulting in their markedly elliptical shapes due to significant flattening (Figure 4g). This type of deformation occurred prior to precipitation of minerals in the vascular cavities, when the bone could still respond plastically within the ductile field (Polonio & López-Martínez 2000). Finally, the plastic deformation observed macroscopically as well as in the bone microstructure would respond, in part, to the fine grain size of the bearing deposits, since a coarse grain size would distribute the lithostatic loads through intergranular contact, attenuating the deformation of the bones (Casal et al. 2019).

Abrasion and bioerosion

The impact of sediment particles mobilized by various erosive agents and friction against the substrate generates a progressive form of mechanical wear known as abrasion in the elements. This phenomenon results in the smoothing and rounding of the edges and processes present in the bones (Fernández-López 2000). No evidence of wear due to abrasion was observed in the elements preserved and recovered from the PS-3 quarry. This finding serves to bolster paleoenvironmental interpretations, particularly those associated with environments characterized by limited to no hydraulic transport. Conversely, no indications of bioerosion, whether occurring pre-burial on the carcass (i.e., scavenging by vertebrates or invertebrates) or during post-burial decomposition processes, are discernible in the examined specimens.

Color and impregnations

A uniform reddish color is exhibited externally by all of the preserved elements, identical to that of the matrix enclosing the remains (reddish pelites). This coloration phenomenon is attributed to the presence of encrustations of calcareous crusts, composed of ferric oxide, which adhere to the surface of the elements. During the technical preparation phase, it was observed that the components display a range of hues varying between whitish and yellowish, a characteristic that is also evident in thin sections of the bones. No mineral impregnations that modify the color of the bones were identified in macroscopic or microscopic observations of thin sections, which is described as category 0 (absence of impregnation) according to the classification system of Tomassini et al. (2010).

Encrusting

Two types of crusting have been identified in the skeletal remains from the PS-3 quarry. The initial crusting has been identified as manganese oxide, with a thickness measuring less than 0.1 mm (Figure 5f). The arrangement of these elements is characterized by irregular forms, giving rise to patterns such as dotted motifs, small dendritic structures, or mottling. The second type has been identified as calcium sulfate (gypsum). The latter is located on specific bone structures, forming a layer with a thickness ranging

between 1 and 2 mm (Figure 5e). In this instance, gypsum functions as an indicator of deposits resulting from the circulation of saturated saline solutions and elevated evaporation rates under predominantly ephemeral conditions. While gypsum by itself does not serve as a definitive indicator of paleoenvironmental characteristics, in this particular instance, its presence is associated with various other variables. This association enables its confident assignment as an indicator of an environment characterized by intense evaporation.

Sedimentary fill

A thorough analysis of the appendicular remains reveals that they all display hollow diaphyses filled with pelitic rocks identified as argillites. These argillites exhibit an identical composition and texture to that of the matrix in which they have been preserved, thereby supporting the hypothesis that the bones could be of autochthonous origin. In sectors where the integrity of bone has been compromised by recent fractures, it has been observed that the sedimentary fill occupying the interior of the bone reproduces the relief of the cavity, replicating highly specific details and generating an internal mold (Figure 5e).

Permineralization

Bones in contact with sediments and fluids within a deposit can undergo a modification of their original mineralogical and geochemical composition (Castaños et al. 2010, Casal et al. 2019). This is controlled–in part–by *pH* and *Eh* conditions, the chemical composition of groundwater, sediment mineralogy, among other factors (Lyman 1994, Casal & Nillni 2020). The permineralization processes identified through the analysis of thin sections of *Thanatosdrakon* bones, observed with a petrographic microscope, suggest that it occurred in two stages. Permineralization is produced by iron oxides that fill all cavities, also impregnating a significant portion of the bone surface. This mineral appeared to be the sole agent responsible for the observed permineralization in the materials (Figure 5c). However, the presence of silica minerals was detected in certain samples. These oxides manifest in a sparse and isolated manner within the analyzed samples, occupying only a limited number of fractures that intersect the iron oxide mineralization (Figure 5h). The presence of silicates is not very common in fossil diagenesis studies of Cretaceous vertebrates preserved in fluvial environments, where carbonates are the main minerals that produce secondary permineralization (e.g., González Riga & Astini 2007, Casal et al. 2013, 2014). However, the absence of carbonate was observed in the analyzed elements.

Consequently, the mineralogical composition of the newly formed and precipitated mineral phases within the vascular cavities, trabeculae, and fractures of the bone remains allows for the estimation of the physical and chemical conditions that prevailed during the processes of lithification and fossilization (*sensu* Merino & Morales 2006). Iron, initially present as an aqueous solution, undergoes precipitation during the early stage of diagenesis under conditions of elevated oxygenation levels and fluctuations in the water table resulting from seasonal variations in climate (*sensu* Meyer 1987, Pereda-Suberbiola et al. 2000, Pfretzschner 2004). The early precipitation of iron oxides, potentially hematite, indicates the influx of Fe-rich solutions under oxidizing conditions, given the stability of hematite in moderately to strongly oxidizing environments (Tucker 1981). Consequently, the mineralogical composition of the bones would have undergone a process of precipitation at a relatively shallow burial depth. The presence of hematite and silica

indicates physicochemical conditions with redox potentials ranging from *Eh* = 0 to +0.1 and *pH* = 7 to 8 within the Plottier Formation.

Finally, it was determined that no fractures were present that exhibited signs of enlargement resulting from crystal growth. Consequently, it is interpreted that the permineralization processes occurred at a depth that generated a sufficiently high confining pressure (Holz & Schultz 1998).

b - Taphonomic Modes:

The concept of taphonomic mode is different and broader than that of taphofacies, as explained by González Riga et al. (2022). A taphonomic mode is 'a recurring pattern of preservation of organic remains in a particular sedimentary context, accompanied by characteristic taphonomic features' (Behrensmeyer 1988:183).

Taphonomic modes facilitate the characterization of preservation patterns, enabling their recognition in other sites and, consequently, prediction. Behrensmeyer & Hook (1992) established taphonomic modes with the purpose of reconstructing the original ecological relationships of the fossil assemblages. To develop this effectively, it is imperative to integrate stratigraphic analyses with taphonomic attributes to characterize a specific preservation. The establishment of taphonomic modes is instrumental in the identification of facies that potentially preserve vertebrate remains under analogous conditions (González Riga et al. 2007). In addition to the aforementioned points, a significant contribution is evident in the clarification of distinctive attributes inherent to the fossil sites. This is of great utility for conducting exhaustive analyses of the fossil records and the identification of biases associated with preservation processes.

González Riga et al. (2022) define three taphonomic modes for floodplains: well-drained floodplain bone assemblage (WDF-BA), variable-drained floodplain bone assemblage (VDF-BA), and poorly-drained floodplain bone assemblage (PDF-BA). Evidently, a floodplain can present these different conditions depending on the size and morphology of the fluvial system, the climatic conditions, and within a fluvial system, depending on whether it is located closer to or further from the main channels. Given the discovery of fossils preserved under variable humidity and subaerial exposure conditions, the PS-3 quarry was assigned to a variably drained floodplain (VDF-BA) taphonomic mode.

According to the parameters proposed by González Riga et al. (2022) (see Table III, taphonomic code), the preservation of specimens UNCUYO-LD 307 and 350 corresponds to a monotaxic site (with multiple individuals of the same taxon). The submode 1, represented by specimen UNCUYO-LD 307, is characterized by disarticulated bones (A5), partially represented (75-25%) (C3), with incipient weathering (W1). Following the code, this taphonomic mode is defined as VDF-BA/M1/A5/C3/W1. Likewise, for this case, it is described as 'variably drained floodplain bone associations that preserve hollow and fragile elements in 3-D, disarticulated but associated skeleton with incipient weathering given a high sedimentation rate' (rapid burial and minimal transport). The submode 2, represented by specimen UNCUYO-LD 350, is characterized by disarticulated bones (A5), isolated bones (C5), and moderate-intense weathering (W3-4). Following the code, this taphonomic mode is defined as VDF-BA/M1/A5/C5/W3-4. Likewise, for this case, it is also described as "variably drained floodplain bone associations that preserve hollow and fragile bones in 3-D, mainly isolated, with moderate weathering due to subaerial exposure".

DISCUSSION

Most taphonomic analyses focus on extrinsic factors associated with sedimentary paleoenvironments and their climatic conditions, which influence the taphonomic history of a given site. While these studies are important because they provide crucial data for defining taphonomic modes, they often overlook intrinsic factors inherent to the nature of the animal that underwent fossilization and upon which extrinsic factors act.

An exhaustive analysis of the *bauplan* of each vertebrate group, with its unique morphological features, is crucial to determining the magnitude of extrinsic factors. In essence, the response of skeletal remains to extrinsic factors varies in each case; that is, within the same paleoenvironmental context, robust sauropods and fragile pterosaurs will respond in different ways.

The analysis of intrinsic factors has been developed, for the first time for Mesozoic vertebrates, in sauropodomorphs, with a particular focus on the anatomical particularities of this diverse lineage of animals. Giant forms have been observed to exceed 30 meters in length, while smaller forms have been documented to reach a mere few meters in length (González Riga et al. 2022). Pterosaurs exhibit morphological characteristics that resemble those previously mentioned, manifesting diminutive forms with a wingspan ranging from centimeters to large-sized specimens exceeding 10 meters (e.g., Wang et al. 2008, Vremir 2010). As has been noted by several authors (e.g., von Meyer 1859, Owen 1870, Bramwell & Whitfield 1974, Padian 1985, Wellnhofer 1991, de Ricqlès et al. 2000), from basally diverging and small-sized pterosaurs to the giants of various lineages that arose in the Cretaceous and generated diverse clades, the bones exhibit a comparable macroscopic structure (i.e., hollow long bones are distinguished by a remarkably thin bony wall, the presence of trabeculae, and a high degree of pneumatization in the vertebrae). In summary, the variations in pterosaur bones – beyond the anatomical particularities that generate synapomorphies and autapomorphies –are fundamentally related to size.

Furthermore, several authors have noted a bias toward the preservation of the skeletons of larger animals (e.g., Behrensmeyer et al. 1979, Behrensmeyer & Dechant Boaz 1980, Arribas & Palmqvist 1998, Germonpré 2003, White & Diedrich 2012). However, the applicability of this phenomenon to disparate vertebrate taxa is not directly evident–e.g., for dinosaurs in general (Dodson 1971) or sauropods in particular (González Riga et al. 2022). Conversely, the pterosaur fossil record shows a notable predominance of small and medium-sized specimens over large and giant forms. As is the case with other vertebrate groups, large-sized animals require a depositional system that generates sufficient sediment to cover their carcasses partially or completely. In this regard, the preservation of large specimens necessitates that the bones demonstrate a high degree of resistance to weathering factors. This ensures that they can withstand weathering conditions for a sufficient duration to allow the carcasses to be covered. However, the results of the present study suggest that this pattern does not seem to be applicable to giant pterosaurs. The results obtained for *Thanatosdrakon* in relation to weathering indicate that the elements demonstrate a low resistance to weathering factors. It is almost obvious that the resistance to weathering, which is low in pterosaurs and higher in sauropods, is due to the bone structure. The former are very thin and hollow, with many bones not exceeding a thickness of 1 or 2 mm. The findings

of this study are not considered to be entirely conclusive due to the fact that they represent a particular case. The paucity of research in this domain underscores the imperative to employ taphonomic methodologies in the examination of diverse quarries to elucidate the questions raised.

The conclusions derived from this analysis can be integrated into deliberations concerning the limited presence of pterosaurs in various sedimentary basins, with the objective of elucidating certain inquiries. In this regard, the limited documentation of pterosaurs in the Argentinean Cretaceous basins of Patagonia merits particular attention. These basins have garnered the scientific community's interest due to the presence of vertebrates, predominantly sauropod and theropod dinosaurs, crocodiles, and turtles. The situation becomes even more complex when considering the characteristics of this fossil record, which is mainly composed of specimens represented by a single isolated and generally incomplete element (see Codorniú & Gianechini et al. 2016 and references therein). *Thanatosdrakon* is integrated into this singular record as the most well represented pterosaur for the Late Cretaceous of Argentina. In the context of the present discussion, a comprehensive analysis of the intrinsic and extrinsic factors that enabled its preservation is imperative to enhance the conceptual framework of the pterosaur record in these outcrops. The analysis conducted revealed that the primary factor contributing to the preservation of *Thanatosdrakon* (specimen UNCUYO-LD 307) was that its death occurred in an environment characterized by a substantial accumulation of sediments (floodplain deposits), which facilitated its progressive burial and, consequently, minimized the exposure of its bones to weathering agents. The specimen UNCUYO-LD 350, as previously referenced, did not undergo the same process due to variations in depositional factors. This aspect, of vital importance for the analysis, follows from the detailed stratigraphic studies and the consequent interpretations of the depositional paleoenvironments. As discussed in the present study, the taphonomic mode of both specimens is associated with the same architectural element: floodplain fines. However, discrepancies can be attributed to variations in sedimentation conditions and exposure duration such as those described in taphonomic submodes.

Floodplain fines (FF *sensu* Miall 1996) are defined as the material that remains suspended in the waters from the overflow of a fluvial system. According to Arche (2010), these facies were deposited in the distal areas of very low-gradient floodplains. The very fine sediment (clay-rich with a minor silt component) is progressively deposited as floodwater evaporates without or with minimal flow. Floodplains are a complex depositional system that exhibits highly variable dynamics depending on the zones considered (proximal or distal), their drainage characteristics (well-drained or poorly drained), the periodicity of water input from the fluvial system, the aridity of the surrounding environment, and other factors. This finding indicates that the paleoenvironmental interpretation of 'floodplain' for a fossil deposit does not provide informative insights regarding taphonomic particularities. This underscores the necessity of conducting meticulous stratigraphic analyses to elucidate the particular characteristics of the quarry. For this reason, this paper defines two taphonomic submodes for the same depositional system. These submodes are characterized by distinct taphonomic processes for each of the *Thanatosdrakon* specimens, resulting from their particular characteristics.

The case study presented herein constitutes the initial phase in the analysis of the variables associated with the fossil preservation of large

pterosaurs in floodplain deposits. A particular emphasis should be placed on the analysis of hypotheses concerning preservational biases that emerge within the pterosaur record. Additionally, they facilitate the establishment of indicators to guide field surveys in outcrops exhibiting these characteristics. In this sense, the results presented in the taphonomic study by Lehman (2021) on *Quetzalcoatlus* remains from the Javelina Formation in the United States and Smith et al. (2023) on pterosaur remains in the Kem Kem Group of Morocco show different taphonomic modes. However, a convergence of findings emerges from both investigations, indicating that the bones were exposed to atmospheric factors for a brief duration, a fact that is in agreement with the conclusions reached in the present study. A comprehensive examination of various preservation cases will facilitate a more profound comprehension of the specific environmental conditions that led to the fossilization of these substantial pterosaurs. This understanding is further enriched by the consideration of the diverse sub-environments in which they existed.

CONCLUSIONS

The results of sedimentary and stratigraphic analyses indicate that the remains of the pterosaurs found at the PS-3 quarry were preserved in reddish pelites, which are interpreted as floodplain deposits resulting from the development of shallow and ephemeral ponds. The minimal energy exerted by these depositional systems led to restricted transport of the bone remains, which do not demonstrate preferential orientations or evidence of abrasion by fluvial transport. Moreover, the arrangement of the elements at the site was found to correspond with five groups that coincide with the proximity of the skeletal elements *in vivo*. Despite its advanced state of decomposition, the carcass retained the anatomical proximity of the bone elements due to the persistence of ligaments, tendons, articular capsules, and muscles. The integration of these structures by soft tissue led to an enhancement in their resistance to dispersal. This factor, in conjunction with the low energy of the depositional system, promoted the autochthonous fossilization of the carcass, with minimal dispersal and transport.

The stratigraphic analysis of the PS-3 quarry, in conjunction with the taphonomic study of the remains found, has enabled the reconstruction of the *Thanatosdrakon* fossilization process. While the history of the PS-3 quarry is unique in its own right, its analysis provides crucial information for understanding the intrinsic and extrinsic processes that led to the accumulation and preservation of the fragile bone remains of vertebrates in this particular paleoenvironment. Additionally, the analysis of plastic deformation processes (which have the potential to generate taphonomic artifacts and obscure the original anatomy of the fossil remains) contributes to the improvement of anatomical descriptions.

The remains of *Thanatosdrakon* were preserved in facies association A (fa-A), as defined for the PS-3 quarry. The association under study is composed of massive, homogeneous red pelites (Fm) where fossiliferous level 1 (FL1) was identified, and reddish and gray pelites with parallel lamination and ripple marks (Fml) where fossiliferous level 2 (FL2) was identified. Paleoenvironmental interpretations indicate changes in depositional conditions, where FL1 is dominated by decantation processes in an extensive playa lake, while FL2 experienced progressive desiccation of the substrate with periodic reactivations of the fluvial system. The taphonomic attributes of the fossil remains are consistent with the characteristics defined for the depositional systems. Based on these

taphonomic and paleoenvironmental results, the PS-3 quarry was assigned to a variably drained floodplain (VDF-BA) taphonomic mode.

The taphonomic history of specimen UNCUYO-LD 307 exhibited partial divergence from that of specimen UNCUYO-LD 350. These disparities enabled the conservation of numerous elements in pristine condition in the smaller specimen, while the larger specimen preserved only the humerus (a component significantly impacted by weathering). During the biostratinomic stage, the carcass of specimen UNCUYO-LD 307 underwent biodegradation, disarticulation, and short-term weathering. The burial process occurred in two stages: an initial stage, immediately following the animal's death and its deposition in a shallow pond, and a final stage, where the bone structures exposed during the decomposition of the carcass were covered by sediment after a brief period of subaerial exposure. During the fossil diagenetic stage, plastic deformation occurred in different elements due to the action of lithostatic pressure. Permineralization is defined as the process by which vascular cavities are filled with hematite, constituting the initial phase of mineralization within the bone tissues. Subsequent examination revealed secondary fracture filling by silicates in certain elements. Brittle deformation manifested in the advanced stages of the replacement of the organic fraction. Finally, encrustation occurred by the deposition of manganese oxides and gypsum on the already fossilized elements.

The carcass of specimen UNCUYO-LD 350, on the other hand, was exposed to environmental conditions characterized by elevated tractive energy, episodic sedimentation by ephemeral flows, and protracted periods of exposure to atmospheric factors. These conditions resulted in the complete disarticulation of the specimen, leaving the various skeletal elements exposed for extended periods, gradually leading to their destruction. The humerus, the sole element of the specimen, was situated at the uppermost limit of the site, a distance of less than 1 meter from the accumulation of remains of specimen UNCUYO-LD 307. The collapse observed in this element indicates the intense weathering that affected specimen UNCUYO-LD 350 compared to specimen UNCUYO-LD 307. The humeri of both specimens–laterally separated by a distance of less than 3 m and located horizontally in the site–were affected differently by the same lithostatic pressure. While one of the elements exhibited only slight deformation in the anteroposterior direction, the other element underwent a complete collapse, resulting in a modification of its structural integrity. This collapse is explained by the weakening of the structure of humerus UNCUYO-LD 350 due to weathering, which affected the integrity of the element and, consequently, its response to pressure.

The particularities in the taphonomic processes described for each specimen allow us to define two taphonomic submodes. The Submode 1, represented by specimen UNCUYO-LD 307, is characterized by disarticulated bones, partially represented (75-25%) with incipient weathering (VDF-BA/M1/A5/C3/W1). While Submode 2, represented by specimen UNCUYO-LD 350, is characterized by disarticulated bones, isolated bones and moderate-intense weathering (VDF-BA/M1/A5/C5/W4). These findings elucidate key aspects of pterosaur preservation and contribute to the understanding of the unique record of these vertebrates in fluvial deposits.

Acknowledgments

We want to thank the authorities of the Facultad de Ciencias Exactas y Naturales de la UNCuyo, Dra. Julieta Aranibar and Lic. Florencia Tarabelli for his constant support of the Laboratorio y Museo de Dinosaurios. We thank the General Coordinator of the Comisión Nacional

del Límite Exterior de la Plataforma Continental (COPLA), Dra. Frida Armas Pfirter and Mr. Marcelo Ancarola (COPLA) for sharing us the bicontinental map of the Argentine Republic and authorizing its use in this publication. We thank the organizers Taissa Rodrigues, Shunxing Jiang and Juliana Sayão for inviting us to participate in the special issue. Finally, we would like to express our sincere gratitude to Dr. Angela Delgado Buscalioni and Dr. Federico Agnolín for their detailed reviews, which enriched and improved this manuscript. Our investigations are funded by the next projects: SIIP-UNCUYO M053-T1 (Director: Dr. Ortiz David), SIIP-UNCUYO M044-T1 (Director Lic. Juan Pedro Coria), SIIP-UNCUYO 06M049-T1 and PIP-CONICET 11220220100021CO (Director: Dr. González Riga).

REFERENCES

AGUIRRE-URRETA MB, CONCHEYRO A, LORENZO M, OTTONE EG & RAWSON PF. 1999. Advances in biostratigraphy of the Agrio Formation (Lower Cretaceous) of the Neuquen Basin, Argentina: ammonites, palynomorphs, and calcareous nannofossils. Palaeogeogr Palaeoclimatol Palaeoecol 150: 33-47.

ALCALÁ L. 1994. Macromamíferos Neógenos de la fosa de Alfambra-Teruel. Instituto de Estudios Turolenses y Museo Nacional Ciencias Naturales, Madrid, 554 p.

ALCALÁ L & ESCORZA CM. 1988. Fracturación en los metápodos de Hipparion. Geogaceta 5: 41-44.

ALCALÁ L & ESCORZA CM. 1998. Modelling diagenetic bone fractures. Bull Soc Géol Fr 169: 101-108.

ANDRES B, CLARK J & XU X. 2014. The earliest pterodactyloid and the origin of the group. Curr Biol 24(9): 1011-1016.

ANDRES B & LANGSTON-JR W. 2021. Morphology and taxonomy of *Quetzalcoatlus* Lawson 1975 (Pterodactyloidea: Azhdarchoidea). J Vertebr Paleontol 41: 46-202.

ARCHE A. 2010. Facies, sedimentología y análisis de cuencas sedimentarias. In: Arche A (Ed), Sedimentología: del proceso físico a la cuenca sedimentaria. Madrid: Consejo Superior de Investigaciones Científicas de España, 15 p.

ARRIBAS A & PALMQVIST P. 1998. Taphonomy and palaeoecology of an assemblage of large mammals: hyaenid activity in the lower Pleistocene site at Venta Micena (Orce, Guadix-Baza Basin, Granada, Spain). Geobios 31: 3-47.

BARRETT PM, BUTLER RJ, EDWARDS NP & MILNER AR. 2008. Pterosaur distribution in time and space: an atlas. Zitteliana 28: 61-107.

BARRIO CA. 1990. Late Cretaceous–Early Tertiary sedimentation in a semi-arid foreland basin (Neuquén Basin, western Argentina). Sedimentary Geology 66: 255-275.

BEARDMORE SR, LAWLOR E & HONE DWE. 2017. Using taphonomy to infer differences in soft tissues between taxa: an example using basal and derived forms of Solnhofen pterosaurs. Sci Nat 104(65). DOI: 10.1007/s00114-017-1486-0.

BEHRENSMEYER AK. 1978. Taphonomic and ecologic information from bone weathering. Paleobiology 4(2): 150-162.

BEHRENSMEYER AK. 1988. Vertebrate preservation in fluvial channels. Palaeogeogr Palaeoclimatol Palaeoecol 63(1-3): 183-199.

BEHRENSMEYER AK. 1991. Terrestrial vertebrate Accumulations. In: Allison PA & Briggs DEG (Eds), Paleobiology: a synthesis. Oxford: Blackwell Scientific Publications, p. 232-235.

BEHRENSMEYER AK & DECHANT BOAZ DE. 1980. The recent bones of Amboseli National Park, Kenya, in relation to East African paleoecology. In: Behrensmeyer AK & Hill AP (Eds), Fossils in the making: vertebrate taphonomy and paleoecology, Chicago: University of Chicago Press, p. 72-92.

BEHRENSMEYER AK & HOOK RW. 1992. Paleoenvironmental contexts and taphonomic modes. In: Behrensmeyer AK, Damuth JD, Dimichele WA, Potts R, Sues H-D & Wing SL (Eds), Terrestrial ecosystems through time. Chicago: The University of Chicago Press, p. 15-136.

BEHRENSMEYER AK, KIDWELL SM & GASTALDO RA. 2000. Taphonomy and paleobiology. Paleobiology 26(4): 103-147.

BEHRENSMEYER AK, WESTERN KD & BOAZ D. 1979 New perspectives in vertebrate paleoecology from a recent bone assemblage. Paleobiology 5: 12-21.

BENNETT SC. 1993. The ontogeny of *Pteranodon* and other pterosaurs. Paleobiology 19(1): 92-106.

BESTWICK J, UNWIN DM, BUTLER RJ, HENDERSON DM & PURNELL MA. 2018. Pterosaur dietary hypotheses: a review of ideas and approaches. Biol Rev 93: 2021-2048.

BESTWICK J, UNWIN DM, BUTLER RJ & PURNELL MA. 2020. Dietary diversity and evolution of the earliest flying vertebrates

revealed by dental microwear texture analysis. Nat Commun 11: 1-9.

BRAMWELL CD & WHITFIELD GR. 1974. Biomechanics of *Pteranodon*. Phil Trans R Soc Lond 267: 503-581.

CALVO O, PORFIRI J, POL D, GONZÁLEZ RIGA BJ, DE LA FUENTE M & ROUGIER GW. 2011. Vertebrados continentales mesozoicos. Actas del XVIII Congreso Geológico Argentino 539-556.

CASAL GA, IBIRICU LM, ALLARD JO, MARTÍNEZ RD, LUNA M & GONZÁLEZ RIGA BJ. 2014. Tafonomía del titanosaurio *Aeolosaurus colhuehuapensis*, Cretácico Superior, Patagonia central, Argentina: un ejemplo de preservación en facies fluviales de desbordamiento. Rev Mex Cienc Geol 31(2): 163-173.

CASAL GA, MARTÍNEZ RD, IBIRICU LM, GONÁLEZ RIGA BJ & FOIX N. 2013. Tafonomía del dinosaurio terópodo *Aniksosaurus darwini*, Formación Bajo Barreal, Cretácico Tardío de Patagonia (Argentina). Ameghiniana 50(6): 571-592.

CASAL GA, MARTÍNEZ R, LUNA M, SCIUTTO JC & LAMANNA M. 2007. *Aeolosaurus colhuehuapensis* sp. nov. (Sauropoda Titanosauria) de la Formación Bajo Barreal, Cretácico Superior de Argentina. Rev Bras Paleontol 10: 53-62.

CASAL GA & NILLNI AM. 2020. Mineralogía y geoquímica de huesos de dinosaurios del Cretácico Superior del Grupo Chubut, Argentina. Rev Soc Geol Esp 33(1): 11-26.

CASAL GA, NILLNI AM, VALLE MN, GONZÁLEZ SVOBODA E, TIEDEMANN C, CIAPPARELLI H, IBIRICU LM & LUIZ MM. 2019. Fósil diagénesis en restos de dinosaurios preservados en depósitos fluviales de la Formación Lago Colhué Huapi (Cretácico Superior). Cuenca del Golfo San Jorge, Argentina. Andean Geol 46(3): 670-692.

CASTAÑOS J, MURELAGA X, CASTELLANOS I, ALONSO-OLAZABAL A, ZULUAGA MC & ORTEGA LA. 2010. Evaluación del grado de diagénesis en huesos fósiles mediante espectroscopía de infrarrojos. Geogaceta 49: 11-14.

CAZAU LB & ULIANA MA. 1973. El Cretácico superior continental de la Cuenca Neuquina. Actas del V Congreso Geológico Argentino 3: 131-163.

CHATTERJEE S & TEMPLIN RJ. 2004. Posture, locomotion and paleoecology of pterosaurs. Spec Pap Geol Soc Am 376: 1-64.

CLADERA G, RUIGOMEZ E, JAUREGUIZAR EO, BOND M & LÓPEZ G. 2004. Tafonomía de la Gran Hondonada (Formación Sarmiento, Edad-mamífero Mustersense, Eoceno Medio) Chubut, Argentina. Ameghiniana 41(3): 315-330.

CODORNIÚ LS & GIANECHINI FA. 2016. The flying reptiles from Argentina: an overview. XXX Jornadas Argentinas de Paleontología de Vertebrados 6: 87-97.

DEAN CD, MANNION PD & BUTLER RJ. 2016. Preservational bias controls the fossil record of pterosaurs. Palaeontology 59(2): 225-247.

DE RICQLÈS AJ, PADIAN K, HORNER JR & FRANCILLON-VIEILLOT H. 2000. Paleohistology of the bones of pterosaurs (Reptilia: Archosauria): anatomy, ontogeny, and biomechanical implications. Zool J Linn Soc 129: 349-385.

DODSON P. 1971. Sedimentology and taphonomy of the Oldman Formation (Campanian), Dinosaur Provincial Park, Alberta (Canada). Palaeogeogr Palaeoclimatol Palaeoecol 10: 21-74.

FERNÁNDEZ-LÓPEZ SR. 2000. Temas de tafonomía. Departamento de Paleontología, Universidad Complutense de Madrid, España, 167 p.

FREY E & MARTILL DM. 1994. A new Pterosaur from the Crato Formation (Lower Cretaceous, Aptian) of Brazil. Neu Jb Geol Paläont Abh 194: 379-412.

GARRIDO AC. 2010. Estratigrafía del Grupo Neuquén: Cretácico superior de Cuenca Neuquina: nueva propuesta de ordenamiento litoestratigráfico. Rev Mus Argentino Cienc Nat ns 12(2): 121-177.

GASPARINI Z, SPALLETTI L & DE LA FUENTE M. 1997. Marine reptiles of a tithonian transgression, western Neuquén Basin, Argentina. Facies and Paleoenvironments. Geobios 30: 701-712.

GASPARINI Z, SPALLETTI L, FERNÁNDEZ M & DE LA FUENTE M. 1999. Tithonian marine reptiles from the Neuquén Basin: diversity and paleoenvironments. Rev Paléobiol 18: 335-345.

GERMONPRÉ M. 2003. Mammoth taphonomy of two fluvial sites from the Flemish Valley, Belgium. In: Reumer JWF, De Vos J & Mol D (Eds), Advances in mammoth research 9, Rotterdam: DEINSEA, p. 171-183.

GONZÁLEZ RIGA BJ. 2002. Estratigrafía y Dinosaurios del Cretácico Tardío en el extremo sur de la Provincia de Mendoza, República Argentina. Tesis Doctoral, Universidad Nacional de Córdoba, 280 p.

GONZÁLEZ RIGA BJ, AGÜERO R, PRIORI E, ALBARRÁN E & ORTIZ DAVID L. 2014a. Preservación de restos fósiles como bienes culturales: experiencias y criterios en la provincia de Mendoza, Argentina. Actas del XIX Congreso Geológico Argentino.

GONZÁLEZ RIGA BJ & ASTINI R. 2007. Fossil preservation of large titanosaur sauropods in overbank fluvial facies: a case study in the Cretaceous of Argentina. J South Am Earth Sci 23(4): 290-303.

GONZÁLEZ RIGA BJ, CALVO JO & PREVITERA E. 2007. Taphonomic analyses of titanosaur sauropods from the Neuquén Basin (Argentina) and their implications in systematic studies. Libro de Resúmenes del IV Jornadas Internacionales sobre Paleontología de Dinosaurios y su entorno, Burgos, España: 73-76 p.

GONZÁLEZ RIGA BJ, CASAL GA, FIORILLO AR & ORTIZ-DAVID LO. 2022. Taphonomy: Overview and New Perspectives Related to the Paleobiology of Giants. In: OTERO A, CARBALLIDO JL & POL D (Eds), South American Sauropodomorph Dinosaurs. Cham: Springer Earth System Sciences, p. 541-582.

GONZÁLEZ RIGA BJ, LAMANNA MC, ORTIZ DAVID LD, CALVO JO & CORIA JP. 2016. A gigantic new dinosaur from Argentina and the evolution of the sauropod hind foot. Scient Rep 6: 19165.

GONZÁLEZ RIGA BJ, ORTIZ DAVID L, LONDERO S, CALVO JO, PORFIRI J & DOS SANTOS D. 2013. Hallazgo de un gigantesco titanosaurio parcialmente articulado del Cretácico Tardío de Mendoza, Argentina. 1st Brazilian Dinosaur Symposium (Ituitaba, Minas Gerais, Brasil), 35 p. (Abstract Book).

GONZÁLEZ RIGA BJ, ORTIZ DAVID L, PORFIRI J, CALVO JO & DOS SANTOS D. 2014b. Preservación y rescate de fósiles de dinosaurios en obras de construcción civil: criterios logísticos y técnicos aplicados en un proyecto minero. Actas del XIX Congreso Geológico Argentino.

HABIB MB. 2008. Comparative evidence for quadrupedal launch in pterosaurs. Zitteliana 28: 65-82.

HOLMBERG E. 1976. Descripción geológica de la Hoja 32c, Buta Ranquil, Provincia del Neuquén. Servicio Geológico Nacional 153: 90. (Buenos Aires).

HOLZ M & SCHULTZ CL. 1998. Taphonomy of the south Brazilian Triassic heryetofauna: fossilization mode and implications for morphological studies. Lethaia 31: 335-345.

HONE DWE & HENDERSON DM. 2014. The posture of floating pterosaurs: Ecological implications for inhabiting marine and freshwater habitats. Palaeogeogr Palaeoclimatol Palaeoecol 394: 89-98.

HOWELL JA, SCHWARZ E, SPALLETTI LA & VEIGA GD. 2005. The Neuquén basin: an overview. In: Veiga GD, Spalletti LA, Howell JA & Schwarz E (Eds), The Neuquén Basin, Argentina: A Case Study in Sequence Stratigraphy and Basin Dynamics. London: Geol Soc Spec Publ 252(1): 1-14.

KELLNER AWA. 1994. Remarks on pterosaur taphonomy and paleoecology. Acta Geol Leopold 39: 175-189.

KELLNER AWA. 2003. Pterosaur phylogeny and comments on the evolutionary history of the group. In: Buffetaut E & Mazin JM (Eds), Evolution and paleobiology of pterosaurs v. 217, London. Geol Soc Spec Publ, p. 105-137.

KELLNER AWA. 2010. Comments on the Pteranodontidae (Pterosauria, Pterodactyloidea) with the description of two new species. An Acad Bras Cienc 82: 1063-1084. https://doi.org/10.1590/S0001-37652010000400025.

KEMP RA. 1999. Solnhofen tetrapod taphonomy. Doctoral thesis, University of Bristol, p. 1-459.

KEMP RA. 2002. Generation of the Solnhofen tetrapod accumulation. Archaeopteryx 19: 11-28.

LEANZA HA, APESTEGUÍA S, NOVAS F & DE LA FUENTE M. 2004. Cretaceous terrestrial beds from the Neuquén basin (Argentina) y their tetrapod assemblages. Cretac Res 25: 1-96.

LEANZA HA & HUGO CA. 1997. Hoja Geológica 3969-III - Picún Leufú, provincias del Neuquén y Río Negro. Inst Geol Rec Nat (SEGEMAR) 218: 135.

LEHMAN TM. 2021. Habitat of the giant pterosaur *Quetzalcoatlus* Lawson 1975 (Pterodactyloidea: Azhdarchoidea): a paleoenvironmental reconstruction of the Javelina Formation (Upper Cretaceous), Big Bend National Park, Texas. J Vertebr Paleontol 41(1): 21-45.

LONGRICH NR, MARTILL DM, ANDRES B & PENNY D. 2018. Late Maastrichtian pterosaurs from North Africa and mass extinction of Pterosauria at the Cretaceous-Paleogene boundary. PLOS Biology 16(3): e2001663.

LÜ J, AZUMA Y, DONG Z, BARSBOLD R, KOBAYASHI Y & LEE YN. 2009. New material of dsungaripterid pterosaurs (Pterosauria, Pterodactyloidea) from western Mongolia and its palaeoecological implications. Geol Mag 146(5): 690-700.

LYMAN RL. 1994. Vertebrate taphonomy. Cambridge: Cambridge University Press, 524 p.

MCGOWEN MR, PADIAN K, DE SOSA MA & HARMON RJ. 2002. Description of *Montanazhdarcho minor*, an azhdarchid pterosaur from the Two Medicine Formation (Campanian) of Montana. PaleoBios 22(1): 1-9.

MERINO L & MORALES J. 2006. Mineralogía y geoquímica del esqueleto de los mastodontes de los yacimientos Batallones 1, 2 y 5: Implicaciones tafonómicas. Est Geol 62: 53-64.

MEYER A. 1987. Phenotypic plasticity and heterochrony in *Cichlasoma managuense* (pisces, cichlidae) and their implications for speciation in cichlid fishes. Evolution 41(6): 1357-1369.

MIALL AD. 1996. The Geology of Fluvial Deposits. Sedimentary Facies, Basin Analysis, and Petroleum Geology. Springer-Verlag, 582 p.

NAISH D & WITTON MP. 2017. Neck biomechanics indicate that giant Transylvanian azhdarchid pterosaurs were short-necked arch predators. Peerj 5: e2908.

NESSOV LA. 1991. Giant flying reptiles of the family Azhdarchidae. II. Paleoenvironment, sedimentological condition of burial. Vestnik Leningradskogo Universiteta, Seriya 7: Geologiya, Geografiya 3(21): 16-24.

ORTIZ-DAVID LD. 2019. Análisis anatómico y filogenético de un pterosaurio gigante de Cuenca Neuquina, Mendoza, Argentina (Unpubl. PhD tesis). Universidad Nacional de Cuyo e ProBiol, Mendoza, Argentina.

ORTIZ-DAVID LD, GONZÁLEZ RIGA BJ, CASAL G, TOMASELLI MB, MERCADO CR, CORIA JP & SÁNCHEZ G. 2024. De autapomorfías a artefactos tafonómicos: análisis sobre la deformación plástica presente en elementos axiales de *Thanatosdrakon Amaru*. In: Actas de la Reunión de Comunicaciones de la Asociación Paleontológica Argentina (RCAPA).

ORTIZ-DAVID LD, GONZÁLEZ RIGA BJ, CORIA JP, TOMASELLI MB, MERCADO CR, SÁNCHEZ TIVIROLI G & GUERRA M. 2021a. Análisis sistemático, filogenético y evolutivo de un nuevo y gigantesco Pterosauria Pterodactiloidea del Cretácico de Mendoza. Libro de Resúmenes del 1er Congreso Interuniversitario I+D+i Mendoza.

ORTIZ-DAVID LD, GONZÁLEZ RIGA BJ & KELLNER AWA. 2018. Discovery of the largest pterosaur from South America. Cretac Res 83: 40-46.

ORTIZ-DAVID LD, GONZÁLEZ RIGA BJ & KELLNER AWA. 2022a. *Thanatosdrakon amaru*, gen. et sp. nov., a giant azhdarchid pterosaur from the Upper Cretaceous of Argentina. Cretac Res 137: 105228.

ORTIZ-DAVID LD, GONZÁLEZ RIGA BJ & KELLNER AWA. 2022b. Anatomical peculiarities of the giant pterosaur *Thanatosdrakon amaru* (Azhdarchidae, Pterodactyloidea) from Upper Cretaceous deposits of Mendoza, Argentina. 82nd Annual Meeting for the Society of Vertebrate Paleontology.

ORTIZ-DAVID LD, GONZÁLEZ RIGA BJ, CANALE JI, TOMASELLI MB, CORIA JP & NOVAS FE. 2023. Anatomía axial del espécimen UNCUYO-LD 308 y comentarios sobre las variaciones en las vértebras de los abelisáuridos del cretácico superior sudamericano. Pe-APA 24(2): R20.

ORTIZ-DAVID LD, GONZÁLEZ RIGA BJ, KELLNER AWA & TOMASELLI MB. 2019a. Análisis ontogenético macro-anatómico e histológico de un gigantesco pterosaurio (Pterodactyloidea – Azhdarchidae) del norte de la Cuenca Neuquina, Mendoza. Libro de Resúmenes del 33° Jornadas Argentinas de Paleontología de Vertebrados (JAPV), p. 65-66.

ORTIZ-DAVID LD, GONZÁLEZ RIGA BJ, KELLNER AWA, TOMASELLI MB, CORIA JP & SÁNCHEZ TIVIROLI G. 2019b. Descripción de un nuevo pterosaurio (Pterodactyloidea – Azhdarchidae) del norte de la Cuenca Neuquina, Mendoza. Libro de Resúmenes del 33° Jornadas Argentinas de Paleontología de Vertebrados (JAPV), p. 66-67.

ORTIZ-DAVID LD, GONZÁLEZ RIGA BJ, KELLNER AWA, TOMASELLI MB, GIOVANETTI MP & MERCADO C. 2019c. Análisis tafonómico de un nuevo pterosaurio (Pterodactyloidea – Azhdarchidae) del norte de la Cuenca Neuquina, Mendoza: un ejemplo de preservación de huesos frágiles en facies de llanuras de inundación. Libro de Resúmenes del 33° Jornadas Argentinas de Paleontología de Vertebrados (JAPV), 66 p.

ORTIZ-DAVID LD, GONZÁLEZ RIGA BJ, TOMASELLI MB, CORIA JP, MERCADO CR, SÁNCHEZ TIVIROLI G, GUERRA M, KELLNER A, CANALE J & NOVAS F. 2021b. Avances de los estudios paleontológicos en el mega-yacimiento Agua del Padrillo (Mendoza, Argentina): fauna de terópodos y pterosaurios. Actas del 16° Encuentro del Centro Internacional de Ciencias de la Tierra, E-ICES 16.

PADIAN K. 1983. A functional analysis of flying and walking in pterosaurs. Paleobiology 9(3): 218-239.

PADIAN K. 1985. The origins and aerodynamics of flight in extinct vertebrates. Paloeontology 28: 413-433.

PALMER C. 2018. Inferring the properties of the pterosaur wing membrane. Geol Soc London Spec Publ 455: 57-68.

PALMER C & DYKE GJ. 2010. Biomechanics of the unique pterosaur pteroid. Proc R Soc B Biol Sci 277: 1121-1127.

PEREDA-SUBERBIOLA X, ASTIBIA H, MURELAGA X, ELORZA JJ & GÓMEZ-ALDAY JJ. 2000. Taphonomy of the Late Cretaceous dinosaur-bearing beds of the Laño Quarry (Iberian Peninsula). Palaeogeogr Palaeoclimatol Palaeoecol 157(3-4): 247-275.

PFRETZSCHNER HU. 2004. Fossilization of Haversian bone in aquatic environments. Comptes Rendus Palevol 3(6-7): 605-616.

POLONIO I & LÓPEZ-MARTÍNEZ N. 2000. Análisis tafonómico de los yacimientos de Somosaguas (Mioceno Medio, Madrid). Colq Paleontol (51): 235-266.

RETALLACK GJ. 2001. Soils of the past. Blackwell, Oxford, p. 1-600.

RICCARDI AC, DAMBORENEA SE & MANCEÑIDO MO. 1999. El Jurásico y Cretácico de la Cordillera Principal y la Cuenca

Neuquina. In: CAMINOS R (Ed), Geología Argentina. Argentina: Instituto de Geología y Recursos Minerales, 29: 419-432. (3. Bioestratigrafía).

SÁNCHEZ ML & HEREDIA S. 2006. Sedimentología y paleoambientes del Subgrupo Río Neuquén (Cretácico Superior) en la quebrada de Las Chivas, departamento Confluencia, provincia de Neuquén. Rev Asoc Geol Argent 61(1): 39-56.

SÁNCHEZ ML, HEREDIA S & CALVO JO. 2006. Paleoambientes sedimentarios del Cretácico Superior de la Formación Plottier (Grupo Neuquén), Departamento Confluencia, Neuquén. Rev Asoc Geol Argent 61(1): 03-18.

SHIPMAN P, BOSLER W & DAVIS KL. 1981. Butchering of giant Geladas in an Acheulian site. Curr Anthropol 22: 257-268.

SMITH RE, MARTILL DM, LONGRICH N, UNWIN DM, IBRAHIM N & ZOUHRI S. 2023. Comparative taphonomy of Kem Kem Group (Cretaceous) pterosaurs of southeast Morocco. Evolving Earth 1: 100006.

TOMASSINI RL, MONTALVO CI, MANERA T & OLIVA C. 2010. Estudio tafonómico de los mamíferos pleistocenos del yacimiento de Playa del Barco (Pehuen Co), provincia de Buenos Aires, Argentina. Ameghiniana 47: 137-152.

TUCKER HA. 1981. Physiological control of mammary growth, lactogenesis, and lactation. J Dairy Sci 64: 1403-1421.

UNWIN DM. 2003. On the phylogeny and evolutionary history of pterosaurs. In: Buffetaut E & Mazin J (Eds), Evolution and paleobiology of pterosaurs, London. Geol Soc Spec Publ 217: 139-190.

UNWIN DM. 2005. Pterosaurs from deep time. New York. Pi press, p. 347.

VON MEYER H. 1859. Zur Fauna der Vorwelt. Vierte Abteilung: Reptilien aus dem lithographischen Schiefer des Jura in Deutschland und Frankreich. H. Keller, Frankfurt am Main, p. 1-114.

VREMIR M. 2010. New faunal elements from the Late Cretaceous (Maastrichtian) continental deposits of Sebeş area (Transylvania). Terra Sebus 2: 635-684.

VREMIR M, KELLNER AWA, NAISH D & DYKE GJ. 2013. A New Azhdarchid Pterosaur from the Late Cretaceous of the Transylvanian Basin, Romania: Implications for Azhdarchid Diversity and Distribution. PLoS ONE 8(1): e54268.

WANG XL, KELLNER AWA, ZHOU ZH & DE ALMEIDA CAMPOS D. 2008. Discovery of a rare arboreal forest-dwelling flying reptile (Pterosauria, Pterodactyloidea) from China. Proc Natl Acad Sci 106(6): 1983-1987.

WELLNHOFER P. 1991. The Illustrated Encyclopedia of Pterosaurs. London: Salamander Books Ltd., 192 p.

WHITE PA & DIEDRICH CG. 2012. Taphonomy story of a modern African elephant *Loxodonta africana* carcass on a lakeshore in Zambia (Africa). Quat Int 276: 287-296.

WILLIAMS CJ, PANI M, BUCCHI A, SMITH RE, KAO A, KEEBLE W, IBRAHIM N & MARTILL DM. 2021. Helically arranged cross struts in azhdarchid pterosaur cervical vertebrae and their biomechanical implications. iScience 24: 102338.

WITTON MP. 2013. Pterosaurs: Natural history, evolution, anatomy. Princeton University Press, 304 p.

WITTON MP & NAISH D. 2008. A reappraisal of azhdarchid pterosaur functional morphology and paleoecology. PLoS ONE 3: e2271.

YRIGOYEN MR. 1991. Hydrocarbon resources from Argentina. In: World Petroleum Congress, Buenos Aires. Petrotecnia 13: 38-54.

How to cite

ORTIZ-DAVID LD, GONZÁLEZ-RIGA BJ, CASAL G, TOMASELLI MB & VIEYRA IF. 2025. Taphonomic analysis of *Thanatosdrakon amaru* (Pterodactyloidea: Azhdarchoidea) and paleoenvironmental reconstruction of the Plottier Formation (Upper Cretaceous, Neuquén Basin), Mendoza, Argentina. An Acad Bras Cienc 97: e20250487. DOI 10.1590/0001-3765202520250487.

Manuscript received on May 8, 2025;
accepted for publication on August 16, 2025

LEONARDO D. ORTIZ-DAVID[1,2]
https://orcid.org/0000-0002-6419-4794

BERNARDO J. GONZÁLEZ-RIGA[1,2,3]
https://orcid.org/0000-0002-6051-472X

GABRIEL CASAL[4]
https://orcid.org/0000-0001-6756-7317

MARÍA BELÉN TOMASELLI[1,2]
https://orcid.org/0000-0003-4150-6609

IMANOL FIGUEREDO-VIEYRA[5]
https://orcid.org/0009-0003-4709-2651

[1]Instituto Interdisciplinario de Ciencias Básicas, Conicet-Uncuyo, Padre Contreras, 1300, Parque Gral. San Martín, 5500 Mendoza, Argentina

[2]Universidad Nacional de Cuyo, Facultad de Ciencias Exactas y Naturales, Museo y Laboratorio de Dinosaurios, Avenida Padre Contreras, 1300, Edificio ECT, Parque General San Martín, 5500 Mendoza, Argentina

[3]Carnegie Museum of Natural History, Research Associate, 4400, Forbes Avenue, 15213 Pittsburgh, U.S.A.

[4]Universidad Nacional de la Patagonia San Juan Bosco, Facultad de Ciencias Naturales y Ciencias de la Salud, Laboratorio de Paleontología de Vertebrados, Ruta prov. Km 4, 9000 Comodoro Rivadavia, Chubut, Argentina

[5]Universidad Nacional de Río Negro, Sede General Roca, Estados Unidos, 750, 8332 Río Negro, General Roca, Argentina

Correspondence to: **Leonardo Daniel Ortiz-David**
E-mail: lortiz@mendoza-conicet.gob.ar

Author contributions

All authors contributed to the development of this work. Leonardo Daniel Ortiz-David was responsible for the general conceptualization of the article. Leonardo Daniel Ortiz-Davidand Bernardo J. González-Riga were responsible for the extraction of fossil remains, stratigraphic studies, and paleoenvironmental interpretations. Leonardo Daniel Ortiz-David was responsible for the technical preparation of the fossils. Leonardo Daniel Ortiz-David, Bernardo J. González-Riga, and María Belén Tomaselli conducted the taphonomic attribute analysis. Leonardo Daniel Ortiz-David and Gabriel Casal performed the thin section and permineralization analysis. Leonardo Daniel Ortiz-David, Bernardo J. González-Riga, and María Belén Tomaselli defined taphonomic modes. Leonardo Daniel Ortiz-David and Imanol Figueredo-Vieyra oversaw the general editing of the article, including the figures and bibliographic citations. María Belén Tomaselli contributed to the language editing, grammar, and overall textual refinement of the manuscript.